Received: 11 February 2022 | Revised: 12 April 2023 | Accepted: 18 April 2023

DOI: 10.1111/bph.16164

RESEARCH ARTICLE

Cognitive dysfunction and impaired neuroplasticity following repeated exposure to the synthetic cannabinoid JWH-018 in male mice

Sabrine Bilel[1] | Erica Zamberletti[2] | Lucia Caffino[3] | Micaela Tirri[1] | Francesca Mottarlini[3] | Raffaella Arfè[1] | Mario Barbieri[4] | Sarah Beggiato[5] | Federica Boccuto[1] | Tatiana Bernardi[6] | Sara Casati[7] | Anna T. Brini[7,8] | Daniela Parolaro[2,9] | Tiziana Rubino[2] | Luca Ferraro[5,10] | Fabio Fumagalli[3] | Matteo Marti[1,11]

[1]Department of Translational Medicine, Section of Legal Medicine and LTTA Center, University of Ferrara, Ferrara, Italy

[2]Department of Biotechnology and Life Sciences (DBSV) and Neuroscience Center, University of Insubria, Busto Arsizio, Italy

[3]Department of Pharmacological and Biomolecular Sciences, 'Rodolfo Paoletti', Università degli Studi di Milano, Milan, Italy

[4]Department of Neurosciences and Rehabilitation, University of Ferrara, Ferrara, Italy

[5]Department of Life Sciences and Biotechnology (SVeB), University of Ferrara, Ferrara, Italy

[6]Department of Environmental Sciences and Prevention, University of Ferrara, Ferrara, Italy

[7]Department of Biomedical Surgical and Dental Sciences, University of Milan, Milan, Italy

[8]IRCCS Galeazzi Orthopedic Institute, Milan, Italy

[9]Zardi-Gori Foundation, Milan, Italy

[10]Laboratory for the Technology of Advanced Therapies (LTTA Centre), University of Ferrara, Ferrara, Italy

Abstract

Background and Purpose: Psychotic disorders have been reported in long-term users of synthetic cannabinoids. This study aims at investigating the long-lasting effects of repeated JWH-018 exposure.

Experimental Approach: Male CD-1 mice were injected with vehicle, JWH-018 (6 mg·kg^{-1}), the CB_1-antagonist NESS-0327 (1 mg·kg^{-1}) or co-administration of NESS-0327 and JWH-018, every day for 7 days. After 15 or 16 days washout, we investigated the effects of JWH-018 on motor function, memory, social dominance and prepulse inhibition (PPI). We also evaluated glutamate levels in dialysates from dorsal striatum, striatal dopamine content and striatal/hippocampal neuroplasticity focusing on the NMDA receptor complex and the neurotrophin BDNF. These measurements were accompanied by in vitro electrophysiological evaluations in hippocampal preparations. Finally, we investigated the density of CB_1 receptors and levels of the endocannabinoid anandamide (AEA) and 2-arachidonoylglycerol (2-AG) and their main synthetic and degrading enzymes in the striatum and hippocampus.

Key Results: The repeated treatment with JWH-018 induced psychomotor agitation while reducing social dominance, recognition memory and PPI in mice. JWH-018 disrupted hippocampal LTP and decreased BDNF expression, reduced the synaptic levels of NMDA receptor subunits and decreased the expression of PSD95. Repeated exposure to JWH-018, reduced hippocampal CB_1 receptor density and induced a

Abbreviations: 2-AG, 2-arachidonoylglycerol; AEA, anandamide; AM 251, 1-(2,4-dichlorophenyl)-5-(4-iodophenyl)-4-methyl-N-(piperidin-1-yl)-1H-pyrazole-3-carboxamide; BDNF, brain-derived neurotrophic factor; DAGLα, diacylglycerol lipase alpha; FAAH, fatty acid amide hydrolase; fEPSP, field excitatory postsynaptic potential; JWH-018, 1-pentyl-3-(1-naphthoyl)indole; MAGL, monoacylglycerol lipase; NAPE-PLD, *N*-acylphosphatidylethanolamine-selective phospholipase D; NESS-0327, *N*-Piperidinyl-[8-chloro-1-(2,4-dichlorophenyl)-1,4,5,6-tetrahydrobenzo-[6,7] cycloheptal[1,2-c]pyrazole-3-carboxamide; OD, optic density; PPI, prepulse inhibition; PSD95, post-synaptic density 95; SCBs, synthetic cannabinoids; SRC, stimulus\response curve; TB5, theta burst: 5 bursts of 5 stimuli; TB10, theta burst: 10 bursts of 5 stimuli; trkB, tropomysin related kinase B; Δ^9-THC, (−)-Δ^9-THC or Dronabinol®.

S. Bilel, E. Zamberletti and L. Caffino contributed equally to the work and can be all considered first authors.

T. Rubino, L. Ferraro, F. Fumagalli and M. Marti share the seniorship.

[11]Collaborative Center for the Italian National Early Warning System, Department of Anti-Drug Policies, Presidency of the Council of Ministers, Rome, Italy

Correspondence
Matteo Marti, Department of Translational Medicine, Section of Legal Medicine and LTTA Center, University of Ferrara, 44121 Ferrara, Italy.
Email: mto@unife.it

Funding information
Department of Anti-Drug Policies, Presidency of the Council of Ministers, Italy; University of Ferrara, Grant/Award Numbers: FAR 2020, FAR 2021; MIUR Progetto Eccellenza, Grant/Award Numbers: PRIN 2017SXEXT5, Progetto Eccellenza

long-term alteration in AEA and 2-AG levels and their degrading enzymes, FAAH and MAGL, in the striatum.

Conclusion and Implications: Our findings suggest that repeated administration of a high dose of JWH-018 leads to the manifestation of psychotic-like symptoms accompanied by alterations in neuroplasticity and change in the endocannabinoid system.

KEYWORDS
BDNF, GABA/glutamate release, hippocampus, JWH-018, LTP, novel object recognition, striatum, synthetic cannabinoid

1 | INTRODUCTION

Synthetic cannabinoids (SCBs) were produced, in the mid-2000s, in clandestine laboratories and have been sold online and in smart shops as smokable 'herbal blends' and 'legal highs' under a variety of brand names such as 'Spice' and 'K2'. These products were labelled as 'not for human consumption', 'incense' or 'for aromatherapy use only'. In 2008, forensic laboratories in Germany and Austria identified the first psychoactive constituent of spice products, the aminoalkylindole JWH-018. Besides their easy access affordability and avoidance of detection in standardized drug tests (Fantegrossi et al., 2014; Fattore & Fratta, 2011; Seely et al., 2012), the growing popularity of spice products is due to their ability to induce far more intense effects than cannabis derivatives together with misinformation regarding their use and toxicity.

Like Δ^9-tetrahydrocannabinol (THC, i.e., the main psychoactive component of cannabis), SCBs bind the central cannabinoid (CB) receptors but with much higher affinity. In fact, JWH-018 binds and activates at low nanomolar concentrations murine, rat and human cannabinoid **CB_1** and **CB_2** receptors (Huffman et al., 1994; Vigolo et al., 2015). Further, JWH-018 has been shown to induce the classical tetrad effects induced by cannabinoid administration, analgesia, catalepsy, hypomotility, and hypothermia (Huffman et al., 2005; Vigolo et al., 2015). Of note, the clinical effects of JWH-018 are mainly mediated by the activation of CB_1 receptor (Davidson et al., 2017).

Beyond the most relevant physical effects following acute SCB consumption that include diaphoresis, psychomotor agitation, palpitations, tachycardia, tachyarrhythmia, convulsion and hyperflexia (Chung et al., 2021; Zawilska & Wojcieszak, 2014), psychotic symptoms have also been reported, including perceptual alterations, illusions, paranoia, catatonia, depersonalization, hallucination, dissociation, anxiety and psychosis (Deng et al., 2018; Fattore, 2016; Orsolini et al., 2019). Interestingly, SCBs can precipitate psychosis in vulnerable individuals, by increasing the risk of developing mental disorders such as schizophrenia (van Amsterdam et al., 2015). Notably SCBs, including JWH-018, are also able to induce psychotic symptoms in subjects with no previous history of psychosis (Deng et al., 2018; Fattore, 2016; Orsolini et al., 2019).

We have recently reported that an acute administration of JWH-018, at low doses (0.01–0.1 mg·kg^{-1}), caused a reduction in sensorimotor as well as prepulse inhibition (PPI) responses in mice (Bilel et al., 2020). This is interesting because decreased PPI is considered an endophenotype of schizophrenia (Swerdlow et al., 2018) as frequently reported in schizophrenic patients. Furthermore, cognitive dysfunctions have been reported clinically; in fact, JWH-018 impairs critical tracking and memory performance in humans, along with psychedelic effects even at moderate doses (Theunissen et al., 2022; Theunissen et al., 2021).

What is already known

- Long-term use of synthetic cannabinoids can cause mental disorders that are precipitated in vulnerable individuals.

What does this study adds

- JWH-018-treated mice exhibit mental dysfunction posing risks for public health arising from repeated drug consumption.

What is the clinical significance

- We provide a mechanism for JWH-018-induced dysfunction that may inform effective and timely interventions.

While the acute effects of SCBs have been extensively reported (for details, see Fattore, 2016), much less is known about the consequences of repeated exposure to this synthetic cannabinoid. Recently, an elegant study from Pintori et al. (2021) employed a low dose of JWH-018 and showed behavioural and biochemical effects 7 days after drug discontinuation suggesting that repeated JWH-018 exposure induces long-lasting neuroplastic effects in the rodent brain. At variance to Pintori et al. (2021), we decided to investigate the effects of an high dose of JWH-018. The reason of our choice stems from a case report showing severe withdrawal symptoms (including hallucinations, cognitive deficit and drug craving) in a 20-year-old male who had consumed the herbal mixture 'Spice Gold' at a high dose on a daily basis (Zimmermann et al., 2009). Accordingly, we employed repeated exposure (7 days) of male adult mice to a high dose (6 mg·kg^{-1}) of JWH-018 and killed them 15 days after the last drug administration. Given the observations reported by Zimmermann et al. (2009) about psychotic symptoms, we incorporated an in vivo battery of behavioural tests indicative for psychotic-like traits (Powell & Miyakawa, 2006) to investigate whether repeated exposure to JWH-018 could be linked to the development of a psychotic phenotype in mice. In addition, because an association between striatum/hippocampus neuroplasticity and mental disorders following SCB exposure has been reported (Basavarajappa & Subbanna, 2014; Davidson et al., 2017; Livny et al., 2018), we investigated the effects of the repeated treatment with JWH-018 on striatal/hippocampal neuroplasticity. In particular, we focused our attention on two critical mediators of neuroplastic mechanisms, that is, the **NMDA** receptor complex and the neurotrophin **BDNF**, whose expression has been found to be altered in animal models of schizophrenia and substance abuse and also in the human equivalent (Delint-Ramirez et al., 2020; Smaga et al., 2021, Errico et al., 2013; Di Carlo et al., 2019). Molecular analyses in hippocampus were coupled with in vitro electrophysiological studies in hippocampal slices to evaluate the effects of the treatment on synaptic excitatory transmission and plasticity. Finally, because the main target of JWH-018 is represented by the endocannabinoid system and alterations in this system have been described in psychosis (Borgan et al., 2021), we also investigated the density of CB_1 receptors as well as the levels of the main endocannabinoid synthetic and degrading enzymes in the striatum and hippocampus.

2 | METHODS

2.1 | Animals

A total of 146 adult male ICR (CD-1®) mice, 30–35 g (Centralized Preclinical Research Laboratory, University of Ferrara, Italy), were group housed (5 mice per cage; floor area per animal was 80 cm^2; minimum enclosure height was 12 cm), exposed to a 12:12-h light–dark cycle (light period from 6:30 AM to 6:30 PM) at a temperature of 20–22°C and humidity of 45%–55% and were provided ad libitum access to food (Diet 4RF25 GLP; Mucedola, Settimo Milanese, Milan, Italy) and water. The experimental protocols performed in the present study were in accordance with the U.K. Animals (Scientific Procedures) Act of 1986 and associated guidelines and the new European Communities Council Directive of September 2010 (2010/63/EU). Experimental protocols were approved by the Italian Ministry of Health (licence no. 956/2020-PR and licence no. 223/2021-PR, CBCC2.46.EXT.21) and by the Animal Welfare Body of the University of Ferrara. Animal studies are reported in compliance with the ARRIVE guidelines (Percie du Sert et al., 2020) and with the recommendations made by the *British Journal of Pharmacology* (Lilley et al., 2020). Authors state that they have complied with the recommendations of the British Journal of Pharmacology on experimental design and analysis (Curtis et al., 2022).

2.2 | Drug preparation, dose selection and repeated JWH-018 administration

JWH-018 was purchased from LGC Standards (LGC Standards S.r.L., Sesto San Giovanni, Milan, Italy), while the CB_1 receptor-preferring antagonist NESS-0327 was purchased from Tocris (Tocris, Bristol, United Kingdom). Each drug was initially dissolved in absolute ethanol (2% final concentration) and Tween 80 (2%) and brought to the final volume with saline (0.9% NaCl). The solution made with ethanol, Tween 80 and saline was also used as vehicle.

To investigate the long-lasting effects of repeated JWH-018 administration, animals were injected with JWH-018 (6 mg·kg^{-1}) or vehicle once a day for seven consecutive days (D1 to D7). Moreover, two groups of animals were treated with the CB_1 receptor-preferring antagonist NESS-0327 (1 mg·kg^{-1}; alone or before the administration of JWH-018) to investigate the involvement of CB_1 receptors in behavioural effects observed after the repeated administration of JWH-018. To this aim, the CB_1 receptor-preferring antagonist (1 mg·kg^{-1}) was administered 20 min before JWH-018 injection. JWH-018 and NESS-0327 were intraperitoneally (i.p.) administered at a volume of 4 µl·g^{-1}. The dose of JWH-018 (6 mg·kg^{-1}) was chosen based on previous studies (Barbieri et al., 2016; Bilel et al., 2020; Ossato et al., 2015; Vigolo et al., 2015) and corresponds to a dosage that addicted users could use for a continuous period and at which most of the psychotic events are observed (Cooper, 2016). The dose of the antagonist was chosen based on a pilot study conducted in our animal model, revealing that the dose of 1 mg·kg^{-1} did not induce any alteration or side effects in mice.

After 15 days (D22) or 16 days (D23) of washout, animals were tested. This long washout period has been selected because previous studies with repeated administration of JWH-018 showed persistent alterations related to the compound after 14 days of washout (Tai et al., 2015). A first group of mice performed the behavioural tests: Mice were treated for 7 days (from day 1 to day 7) once a day with vehicle, JWH-018 (6 mg·kg^{-1}), NESS-0327 (1 mg·kg^{-1}) and NESS-0327 (1 mg·kg^{-1}) + JWH-018 (6 mg·kg^{-1}). Mice were divided into five main groups: two that performed the tests on day 22 (D22) and three that performed the tests on day 23 (D23). On D22, one group (Table S1, G1) of animals was tested for spontaneous locomotion, drag and accelerod test in the morning (9:00 to 12:00 AM) and was also tested on the tail suspension test in the afternoon (2:00–4:00 PM); the second group of mice (Table S1, G2)

was tested for novel object recognition (NOR) in the morning (9:00 to 12:00 AM) and in the social dominance test in the afternoon (2:00–4:00 PM). In vivo experiments were conducted blind by trained observers working together in pairs (Ossato et al., 2016). Moreover, we evaluated the long-term effects of repeated JWH-018 administration on dopamine. On D23 the third group of mice (Table S1, G3) was tested on startle/PPI in the morning (9:00 to 12:00 AM) and was also used for in vitro electrophysiological experiments during the afternoon (Table S1). The fourth group of mice (Table S1, G4) were divided into two different subgroups: One was used for the in vivo microdialysis (Table S1, G4a), and the second (Table S1, G4b) killed and hippocampal and striatal areas were dissected. Dissections were performed according to the mouse atlas of Paxinos and Franklin; the hippocampi were dissected according to Spijker (Spijker, 2011). Lastly, the fifth group of mice (Table S1, G5) was used to evaluate the long-term effects of repeated JWH-018 administration on AEA and 2-AG levels in mice striatum.

We reported a schematic representation of the experimental protocol in Figure 1, and the groups and relative numbers of animals used in every specific test are reported is Table S1.

2.3 | Behavioural studies

2.3.1 | Spontaneous locomotor activity

Spontaneous locomotor activity was measured by using the ANY-maze video-tracking system (Ugo Basile, application version 4.99 g Beta, Milan, Italy). As previously reported, the mouse was placed in a square plastic cage (60 × 60 cm) located in a sound- and light-attenuated room and the motor activity (distance travelled (m), time spent in the central and peripheral area (s), entries in the central and peripheral area (no. of entries), rotations of animal's body (no. of rotations), maximum and average running speed ($m \cdot s^{-1}$)) were analysed every 5 min and monitored for 240 min. Four mice were monitored at the same time in each experiment (Bilel et al., 2020; Canazza et al., 2016; Ossato et al., 2015; Ossato et al., 2017). To avoid olfactory cues, cages were carefully cleaned with a dilute (5%) ethanol solution and washed with water between each trial. All experiments were performed between 9:00 AM to 1:00 PM.

2.3.2 | Novel object recognition test

The novel object recognition (NOR) test was chosen as it represents a 'pure' working memory task, which does not involve the retention of a rule, but it is entirely based on the spontaneous exploratory behaviour of rodents toward objects (Ennaceur et al., 1997).

As previously reported (Barbieri et al., 2016), the test was conducted in three phases: habituation, familiarization and choice. Firstly, CD-1 mice were subjected to a 3-day habituation phase, conducted by placing each animal into the novel object recognition (NOR) test chamber (a square open field 60 cm × 60 cm × 40 cm, dark PVC plastic box) located in a dimly lit (50 lux), sound-attenuated and acclimatized room. Mice were allowed to explore freely for 20 $min \cdot day^{-1}$. No objects were placed in the box during the habituation trial. Twenty-four hours after last habituation period, the familiarization trial was conducted by placing the mouse in the field in which two identical objects (A, A) were positioned on the corners of the arena

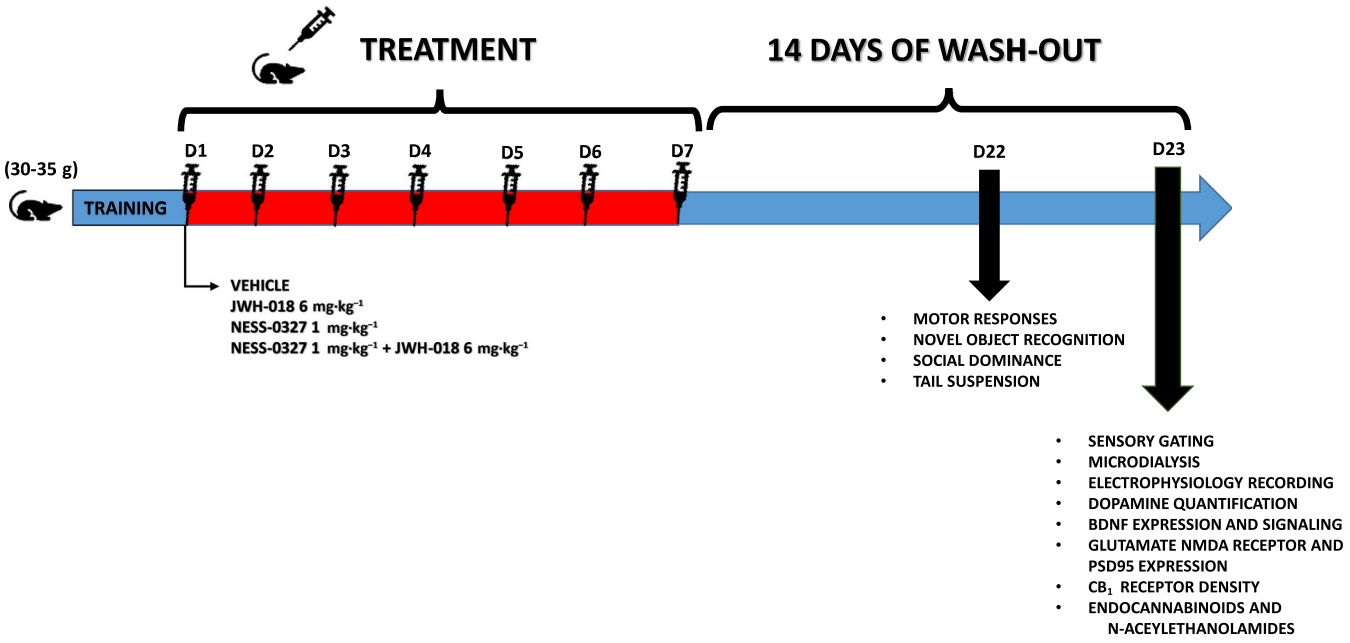

FIGURE 1 Schematic representation of protocol used for the experiments. Mice were treated for 7 days (from day 1 to day 7) once a day with vehicle, the synthetic cannabinoid JWH-018 (6 $mg \cdot kg^{-1}$), the CB_1 receptor antagonist NESS-0327 (1 $mg \cdot kg^{-1}$) or NESS-0327 (1 $mg \cdot kg^{-1}$) + JWH-018 (6 $mg \cdot kg^{-1}$). After 15 (D22) or 16 (D23) days of washout, we performed behavioural, electrophysiological, neurochemical and molecular analysis.

approximately 6 cm from the walls. Mice were placed at the mid-point of the wall opposite to the objects and allowed to explore them for 15 min. After 1 h, one of the two familiar objects (A) was replaced with a new one (novel; B), different in shape, dimension and colour. Each mouse was then placed in the apparatus and left free to explore the objects (A and B) for 5 min. After 1 h from the 'object' recognition test, we performed the 'spatial' recognition test. In the spatial choice test, the mice explored the open field for 5 min in the presence of two familiar object (A and B). Object A is kept in the same previous position, while object B has been positioned at a different point from its previous position (spatial memory). Exploration was defined as the time (s) during which the mouse nose was in contact with the object or directed toward it at a distance ≤ 2 cm. The mouse going around the object was not considered as exploratory behaviour.

All experiments were performed using the ANY-maze video tracking system (Ugo Basile, application version 4.99 g Beta) and subsequently analysed by an observer blind to the mouse treatment and to which object was the novel one. Exploration time of familiar (A) and novel (B) object (or familiar object but placed in a different position) was measured. The novel object preference was quantified as recognition index (RI) calculated as (novel B − familiar A)/(novel B + familiar A). Using this metric, scores approaching zero reflects no preference (impairment of recognition memory), positive values reflect preference for the novel object (good recognition memory) while negative numbers reflect preference for the familiar (impairment of recognition memory). Moreover, the total exploration time (s) spent by the animal in the choice phase at 2 h (familiar A + novel B) and 24 h (familiar A + novel C) was calculated to investigate the effect of drugs on object exploration.

The objects to be discriminated by mice were seven sets of novel and familiar objects of different material (plastic, glass or ceramic), shape (cube, parallelepiped and cylinder), dimension (height: 3–8 cm; width: 6–8) and colour (light yellow, red and blue). The object weight was such that it could not be displaced by mice. To avoid olfactory cues, objects and apparatus were carefully cleaned with a dilute (5%) ethanol solution and water between animal trials and also between familiarization and choice phase.

2.3.3 | Tail suspension test

The tail suspension test (TST) is one of the most widely used models for assessing antidepressant-like behaviours in mice. It was suggested in many studies that the endocannabinoid system, in particular the cannabinoid receptors (CB_1 and CB_2) play a significant role in the pathophysiology of depression and stress/anxiety disorders (Li et al., 2019; Maldonado et al., 2020; Poleszak et al., 2020; Smaga et al., 2017). We investigated in a previous study the acute effects of Δ9-THC and JWH-018 and its halogenated derivatives on the tail suspension test as a first investigation to reveal their possible actions in affecting stress/anxiety in mice, as suggested by literature (Barbieri et al., 2016). The use of the tail suspension test in this study is therefore aimed to fill the gap in knowledge on the effect of prolonged administration of JWH-018 in mice in response to stress (tail suspension test) and to reveal a possible endophenotypic alteration when compared with vehicle-treated mice (Li et al., 2019).

The tail suspension test (TST) was performed according to the method previously reported (Barbieri et al., 2016). Briefly, CD-1 mice, both acoustically and visually isolated, were suspended 50 cm above the floor by an adhesive tape placed approximately 1 cm from the tip of the tail. Immobility time was recorded during a 6-min period (Barbieri et al., 2016). The mice were considered immobile only when they hung passively and were completely motionless (Porsolt et al., 1977). For tail suspension test (TST) evaluation, all experiments were videotaped, and the ANY-maze video tracking system was used (Ugo Basile, application version 4.99 g Beta) and scored by an observer blind to the treatment.

2.3.4 | Social dominance test

The tube test for social dominance is a common test for assessing social behaviour in mice (Lijam et al., 1997). In this test, two mice are released into opposite ends of a plastic tube (3.7 cm inner diameter and 30.5 cm in length) and meet in the middle. One mouse will typically push the other out of the tube. The match ended when one mouse completely retreated from the tube. The mouse remaining in the tube was designated the winner or more dominant mouse (score = 1) and the retreating mouse was the loser (score = 0). Matches lasting more than 5 min or in which the mice crossed over each other were not scored. Each mouse performed three matches against the mouse of the different cage.

2.3.5 | Evaluation of startle reactivity and prepulse inhibition

Mice underwent the pre-pulse inhibition (PPI) test for measuring the acoustic startle reactivity in startle chambers (Ugo Basile) consisting of a sound-attenuated, lighted and ventilated enclosure holding a transparent non-restrictive Perspex® cage (90 × 45 × 50 mm). A loudspeaker mounted laterally to the holder produced all acoustic stimuli. Peak and amplitude of the startle response were detected by a load cell. At the onset of the startling stimulus, 300-ms readings were recorded and the wave amplitude evoked by the movement of the animal startle response was measured. Acoustic startle test sessions included startle trials (pulse-alone) and prepulse trials (prepulse +pulse) consisting, respectively, of a 40-ms 120-dB pulse and of a 20-ms acoustic prepulse+80-ms delay and then a 40-ms 120-dB startle pulse (100-ms onset-onset). There was an average of 15 s (range: 9–21 s) between the trials. Animals were placed in the startle chambers 5 min after drug administration; the entire PPI test lasted 20 min. Each session began with a 10-min acclimation period with a 65-dB broadband white noise that remained present throughout the session. The test session contained 30 trials composed by pulse-alone and

prepulse+pulse trials (with two different prepulses of 75-dB and 85-dB) presented in a pseudorandomized order. PPI responses were recorded at D22 (15 days of drug washout) after vehicle or JWH-018 injections and were expressed as percentage decrease in the amplitude of the startle reactivity caused by the presentation of the prepulse (% PPI).

2.4 | Electrophysiological studies in hippocampal slices

2.4.1 | Tissue preparation

The hippocampal transverse slice model was used to investigate the long-lasting effects of repeated JWH-018 administration on synaptic excitatory transmission and plasticity at D23 washout from JWH-018 or vehicle. Six mice were used from each experimental group. Procedures for tissue preparation are the same as described in Barbieri et al., 2016. In brief, after mouse decapitation the brain was quickly extracted, hippocampus isolated and placed in ice-cold artificial cerebrospinal fluid (aCSF), of the following composition (in mM): NaCl, 126; KCl, 2; KH_2PO_4, 1.25; $NaHCO_3$, 26; $MgSO_4$, 2.0; $CaCl_2$, 2.5; D-glucose 10. All solutions were saturated with 95% O_2/5% CO_2. Transverse hippocampal slices (425 μm thick) were cut with a tissue chopper, then placed for almost 90 min in a Haas style incubation chamber for recovery until recording.

2.4.2 | Electrophysiological recording

Before recording, CA1 and CA3 areas were surgically disconnected. A single slice was then transferred into a submerged-type recording chamber (3 ml total volume) and continuously superfused (3.0 ml·min^{-1}) with warmed (32–33°C) aCSF. WINLTP 2.10 computer software, Bristol, UK (Anderson & Collingridge, 2007) was used for stimulus triggering, PC recording and analysis. Synaptic responses of CA1 pyramidal neurons were elicited by electrical stimulation of the Schaffer collateral/commissural pathway. Single stimulation pulse (80 μs duration; 0.05 Hz) was delivered by means of a concentric bipolar electrode (o.d. 125 μm, FHC, USA) connected to a Grass S11 stimulator driving a PSIU6 constant current stimulus isolation unit. To record, the fEPSPs were recorded using borosilicate glass electrodes fabricated using a P2000 Sutter puller (Sutter Instruments) and filled with aCSF (1.5 ± 0.5 MΩ), placed in the distal third of the stratum radiatum. Distance between the stimulating and recording electrodes was 200–300 μm. To achieve the maximal fEPSPs response, the depth of the recording electrode was adjusted. Recorded potentials were amplified (Axoclamp2A DC-coupled - Cyberamp 320, Molecular Devices, Sunnyvale CA, USA) and filtered (5.0 kHz) prior to A/D conversion. Once a stable synaptic response had been attained for at least 20 min, a stimulus response curve (SRC) was generated as previously described (Zucchini et al., 2008). From SRCs were extrapolated the fold-increase in input stimulus intensity necessary for evoking a half-maximal response, parameter index of synaptic pathway excitability and the stimulation intensity yielding a fEPSP ~40%–45% of the maximal achievable was set then held constant throughout the experiment. To evaluate modifications of synaptic plasticity, we induced LTP by mean of the theta-burst (TB5) stimulation paradigm. The TB5 with respect to other stimulation paradigms presents several advantages, overall, a stable and non-decremental LTP and higher sensitivity to the different experimental manipulations (Larson & Munkácsy, 2015). TB5 consists of a single train of five bursts of five stimuli (100 Hz intraburst frequency, 5 Hz burst frequency). To allow the correct measurement of TB5-induced LTP in the same slice, a two-pathway stimulation protocol was applied (see Section 2.9). Namely, two independent synaptic inputs were activated in the Schaffer collateral area (identified as 'control' and 'test'), represented by two stimulating electrodes located on opposite sites relative to the recording electrode (Barrionuevo & Brown, 1983) (see scheme in Figure 8 for electrode placement). Input pathways were alternately stimulated every 15 s. At the end of the experiment (45 min after TB5), test pathway was activated with TB10 stimulation (10 bursts of five stimuli, 100 Hz intraburst frequency and 5 Hz burst frequency) to evoke the maximally achievable potentiation as a control for slices viability (Barbieri et al., 2016; Morini et al., 2011). The response was followed for 15 min, and average of values in the last 2 min was the reference parameter to evaluate the maximal potentiation achievable. The magnitude of maximal potentiation obtained with TB10 stimulation was also used in additional analyses to calculate TB5 stimulation-induced LTP as a fraction of maximally inducible potentiation in each slice, thereby minimizing variability due to differences in LTP susceptibility between preparations.

2.5 | Microdialysis

2.5.1 | Surgery and dialysate sample collection

On the day of surgery, the animals, kept under isoflurane anaesthesia (1.5% mixture of isoflurane and air, Ugo Basile), were mounted in a David Kopf stereotaxic frame (Tujunga, CA, USA) with the upper incisor bar set at −2.5 mm below the interaural line. After exposing the skull and drilling a burr hole, a microdialysis probe (2-mm membrane length; cut-off 6000 Da; CMA-11, CMA/Microdialysis, Solna, Sweden) was positioned on top of the dorsal striatum using the following coordinates from Bregma (AP: + 0.3, L: 2.2 mm from the midline, V: −4.4 mm below the dura), according to the atlas of Franklin and Paxinos (2008) and secured to the skull with an anchor screw and acrylic dental cement. After surgery, the animals were housed individually in microdialysis chambers.

On the day after surgery, the probe was connected to a microperfusion pump (CMA 100; Carnegie Medicin, Stockholm, Sweden) set to a speed of 1.5 μl·min^{-1} and perfused with Ringer solution containing (in mM): NaCl, 144; KCl, 4.8; $MgSO_4$, 1.2; $CaCl_2$, 1.7; pH 6.7. Perfusates were collected every 20 min and, to achieve stable dialysate glutamate, collection of samples started 300 min after the onset of

perfusion. In a first series of experiments, after three stable basal values were obtained, the probe was perfused (10 min) with an isotonic Ringer solution containing 50 mM KCl. This medium was then replaced with the original one and further 3 samples were collected. In a second series of experiments, after three stable basal values were obtained, mice were gently disturbed with a spatula for 5 min and further three samples were collected.

Following each experiment, the brain was removed from the skull, and the position of the dialysis probe was verified using 30-µm-thick coronal cryostat sections. Only animals in which the probe was correctly located were included in the study.

2.5.2 | Glutamate analysis

Glutamate levels in the perfused samples were measured by HPLC with fluorimetric detection. Briefly, 25 µl were transferred into glass microvials and placed in a temperature-controlled (4°C) Triathlon autosampler (Spark Holland, Emmen, the Netherlands). Thirty microlitres of *o*-phthaldialdehyde/mercaptoethanol reagent were added to each sample, and 30 µl of the mixture were injected onto a Chromsep analytical column (3 mm inner diameter, 10 cm length; Chrompack, Middelburg, the Netherlands). The column was eluted at a flow rate of 0.75 ml·min^{-1} (Beckman125 pump; Beckman Instruments, Fullerton, CA, USA) with a mobile phase containing 0.1 M sodium acetate, 10% methanol and 2.2% tetrahydrofuran (pH 6.5). Glutamate was detected by means of a Jasco fluorescence spectrophotometer FP-2020 Plus (Jasco, Tokyo, Japan). The retention times of glutamate was ~ 3.5 min.

2.6 | Ex vivo evaluation of striatal dopamine content

2.6.1 | Tissue collection

Animals were killed using an anaesthetic overdose of isoflurane. The brains were rapidly removed, and the striata were rapidly dissected out, weighed and frozen on dry ice and stored at −80°C until the day of the assays.

2.6.2 | UPLC-MS/MS method

The striata of each mouse was added to 250 µl of $HClO_4$ 0.3 M frozen solution. The mixtures were sonicated in a cold ultrasonic bath (BRANSON 1510, Bransonic, Danbury, USA) and centrifuged at 14,000 rpm, 16,464 g, for 30 min at 4°C (MPW 65R, MPW MED. INSTRUMENTS, Warsow, Poland). The supernatant was collected with great caution (to avoid pellet) and injected into high performance liquid chromatography (HPLC; Gemechu et al., 2018).

The separation method was a linear gradient of 5.1 min: solvent A (0.1% formic acid water) 95% at gradient started at 4.0 min to 5% and remained constant for 1 min, returning to 95% at 5.10 min with a flow rate of 0.4 ml·min^{-1}. The Acquity column UPLC HSS C18 1.8 µm (2.1 × 150 mm) was brought into equilibrium at the gradient start conditions before the next injection. The acquisition was performed in ion positive MRM mode for the parent ion 154,0843 m/z with its fragments 91,0083 m/z (cone voltage 22 V, collision energy 24 V) and 137,0258 m/z (cone voltage 22 V, collision energy 8 V). Retention time 0.63 min. Instrument: Acquity H-Class and Xevo TQD Waters Mass Spectrometer (Waters Corporation, Milford, USA).

2.7 | Ex vivo evaluation of endocannabinoid levels in the striatum

2.7.1 | Chemicals

Ultrapure water, acetonitrile, dichloromethane, isopropanol, methanol, and hydrochloride acid were of analytical grade and purchased from Carlo Erba (Milan, Italy). Formic acid (98%100%) was purchased from Sigma–Aldrich (Milan, Italy).

2.7.2 | UHPLC–MS/MS analysis of endocannabinoids and N-acylethanolamides

Anandamide and 2-arachidonoylglycerol quantification was performed using a QTRAP 5500 triple quadrupole linear ion trap mass spectrometer (Sciex, Darmstadt, Germany) coupled with an Agilent 1200 Infinity pump ultra-high pressure liquid chromatography (UHPLC) system (Agilent Technologies, Palo Alto, CA, USA), following recently validated methods [doi.org/10.3390/biom10091302]. Compounds were separated on a Kinetex UHPLC XB-C18 column (100 × 2.1 mm i.d., 2.6 p.s.) (Phenomenex, Torrance, CA, USA) using a linear gradient elution of 0.1% formic acid in water (mobile phase A) and methanol/acetonitrile (5:1; v/v) (mobile phase B). Briefly, 125 µl of homogenized tissue was extracted following a liquid–liquid extraction procedure (4 ml of dichloromethane/isopropanol 8:2; v/v), after a protein precipitation with cold acetonitrile (1 ml). The supernatant was separated and dried under a gentle stream of nitrogen. The residue was reconstituted in 60 µl methanol, and 3 µl aliquot was injected into the UHPLC/MS–MS system for lipids determination. Data acquisition and processing were performed using Analyst 1.6.2 and MultiQuant 2.1.1 Software (Sciex, Darmstadt, Germany), respectively.

2.8 | Molecular analyses

2.8.1 | Western blot analyses of BDNF-related system, glutamate signalling and endocannabinoid-related enzymes

The striata and hippocampi were homogenized in a glass–glass potter using a cold buffer containing 0.32 M sucrose, 1 mM Hepes solution,

0.1 mM EGTA, 0.1 mM PMSF, pH = 7.4, in the presence of a complete set of protease inhibitors and a phosphatase inhibitor cocktail. Crude synaptosomal fraction was prepared as previously described (Caffino et al., 2017). The homogenized tissues were centrifuged at 1000 g for 10 min; the resulting supernatant was centrifuged at 9000 g for 15 min to obtain the pellet corresponding to the crude synaptosomal fraction, which was re-suspended in a buffer containing 20 mM Hepes, 0.1 mM DTT, 0.1 mM EGTA, in the presence of a complete set of protease inhibitors and a phosphatase inhibitor cocktail. Total proteins were measured in the whole homogenate and in the crude synaptosomal fraction by the Bio-Rad Protein Assay, using bovine serum albumin as the calibration standard (Bio-Rad Laboratories, Milan, Italy). The immuno-related procedures used comply with the recommendations made by the *British Journal of Pharmacology* (Alexander et al., 2018).

To evaluate the expression of glutamate-related proteins and of the BDNF-related system, equal amounts of protein were run under reducing conditions on the criterion TGX precast gels (Bio-Rad Laboratories, Milan, Italy). To evaluate the expression of endocannabinoid-related enzyme, equal amounts of total protein lysates (30 μg) were run on a 10% SDS-polyacrylamide gel. Then proteins were electrophoretically transferred onto polyvinylidene difluoride membranes (GE Healthcare, Milan, Italy).

Blots were blocked for 1 h at room temperature with 10% non-fat dry milk in TBS + 0.1% Tween-20 buffer, incubated with antibodies against the phosphorylated forms of the proteins and then stripped and reprobed with the antibodies against corresponding total proteins.

The conditions of the primary antibodies were the following: mouse monoclonal mBDNF (1:500, Icosagen, Estonia); rabbit polyclonal anti phospho-trkB Y706 (1:200, Novus Biologicals, USA), rabbit polyclonal anti total trkB (1:1000, Cell Signaling Technology, USA); rabbit polyclonal anti phospho-Akt S473 (1:1000, Cell Signaling Technology); rabbit polyclonal anti total Akt (1:1000, Cell Signaling Technology); mouse monoclonal anti Arc/Arg3.1 (1:500, BD Transduction Laboratories, USA), rabbit polyclonal anti **GluN1** (1:1000, Invitrogen, Carlsbad, CA, USA), rabbit polyclonal anti **GluN2B** (1:1000, Cell Signaling Technology), rabbit polyclonal anti **GluN2A** (1:1000, Invitrogen), mouse monoclonal anti PSD-95 (1:4000, Cell Signaling Technology), rabbit polyclonal anti-CB1 (1:1000; Cayman Chemical, USA), rabbit polyclonal anti-**FAAH** (1:1000; Cayman Chemical, USA), rabbit polyclonal anti-**MAGL** (1:1000; Cayman Chemical, USA), rabbit polyclonal anti-**NAPE-PLD** (1:3000; Cayman Chemical, USA) and goat polyclonal anti-**DAGLα** (1:1000; AbCam, UK) and mouse monoclonal anti β-Actin (1:10,000, Sigma-Aldrich, Italy). Bound antibodies were detected with horseradish peroxidase (HRP) conjugated secondary anti-rabbit, anti-mouse or anti-goat antibodies (1:1000–5000; Santa Cruz Biotechnology, USA) for 1 h at room temperature.

Expression levels of every single protein run on the same gel was normalized using its own β-Actin loading control, which was detected by evaluating the band density at 43 kDa. Each set of proteins (presented in Figure 9, Figure 10 and Figure 11) was run in the same WB assay, thus only one band of β-actin was represented. To evaluate the expression of glutamate-related proteins and of the BDNF-related system, optic density (OD) of immunocomplexes was visualized by chemiluminescence using the Chemidoc MP Imaging System (Bio-Rad Laboratories). Gels were run 2 times each and the results represent the average from 2 different runs. We used a correction factor to average the different gels: correction factor gel 2 = average of (OD protein of interest/OD β-actin for each sample loaded in gel 1)/(OD protein of interest/OD β-actin for the same sample loaded in gel 2) (Caffino et al., 2020). To evaluate the expression of endocannabinoid-related enzyme, bound antibodies were detected with a GBOX XT camera (Syngene, Cambridge, UK). Optical density of the bands was quantified using ImageJ software (NIH, Bethesda, MD, USA) and normalized to β-actin. To allow comparison between different blots, the density of the bands was expressed as percentage of vehicle.

2.8.2 | [^{3}H]CP-55940 receptor autoradiographic binding

Brains were rapidly removed after decapitation, frozen in liquid nitrogen for 1 min and stored at −80°C until processing; 20-μm-thick coronal sections were cut on a cryostat and thaw-mounted on gelatin-coated slides. Slides were incubated for 2.5 h at 37°C with 10 nM [^{3}H]CP-55940 (Perkin Elmer Life Sciences, Milan, Italy) in binding buffer [50 mM Tris–HCl, pH 7.4, 5% bovine serum albumin (BSA)]. Adjacent cerebral sections were incubated in parallel with 10 ml CP-55940 to assess non-specific binding. Sections were washed for 1 h at 4°C in a buffer containing 50 mM Tris–HCl pH 7.4, 1% BSA-buffer and rinsed for 3 h in the same conditions. They were then dipped in 50 mM Tris–HCl buffer (pH 7.4) for 5 min and then in distilled water. Once dried, the sections were exposed to Kodak Biomax MR films (Perkin Elmer Life Sciences, Milan, Italy) for 14 days to generate autoradiograms. Intensity of autoradiographic films was assessed by measuring grey levels using Image-Pro Plus 7.0 (MediaCybernetics, Silver Spring, USA). Each area of both sides of the brain was traced with the mouse cursor using the Paxinos and Watson rat brain atlas as reference. Grey level of densitometric measurements calculated after subtraction of the film background density was determined using tritium standards for receptor binding (^{3}H Microscales, Amersham Pharmacia Biotech, Braunschweig, Germany) as previously reported (Zamberletti et al., 2012).

2.9 | Data presentation and statistical analysis

The data and statistical analysis comply with the recommendations of the *British Journal of Pharmacology* on experimental design and analysis in pharmacology (Curtis et al., 2022). All animals tested were treated as independent values, and there were no technical replicates.

The Kolmogorov–Smirnov test was employed to determine normality of residuals: No significant variance in homogeneity was found.

Data are expressed in absolute values or in percent changes and are presented as the mean ± SEM or SDM when indicated.

Statistical analysis for in vivo behavioural results was performed on absolute data by one-way or two-way repeated measure (RM) analysis of variance (ANOVA), as specified in figure captions. Post-hoc tests were run only if F achieved P<0.05 and there was no significant variance inhomogeneity, and Bonferroni post hoc tests were performed to determine group differences.

The amount of PPI was calculated as a percentage score for each prepulse + pulse trial type: %PPI = 100 − {[(startle response for prepulse + pulse trial)/(startle response for pulse-alone trial)] × 100}. Startle magnitude was calculated as the average response to all the pulse-alone trials.

For the in vitro electrophysiological experiments, the fEPSP amplitude was defined as the slope of the initial falling phase of the electrical response recorded following the afferent volley, and measured by linear regression in the region between 30% and 70% of the fEPSP. To calculate TB5 stimulation-induced synaptic potentiation in test pathway independent of possible excitability rundown affecting both inputs, we used the following procedure: For each experiment, the measured fEPSP slopes recorded from both inputs were recorded (see Section 3.4). The normalized values of control (non-potentiated) input were then subtracted from the corresponding values of the test (potentiated) input to obtain the net potentiation (i.e., LTP). Steady-state values of net potentiation produced by TB5 stimulation were obtained by averaging the values of the 11 consecutive responses recorded over the 5 min period between 40 and 45 min after TB5 stimulation. The maximally achievable potentiation was calculated by averaging the values of five responses over the 2 min period between 13 and 15 min after TB10 stimulation. Statistical difference was calculated by unpaired Student's *t*-test.

For the microdialysis data, the mean ± SEM of the three samples collected prior to KCl perfusion or mouse-disturbing has been used to calculate basal extracellular glutamate levels. The effects of KCl perfusion or mouse gentle-disturbing were reported as the percentage of the respective basal extracellular glutamate levels. The statistical analysis was carried out by Student's *t*-tests.

Ex vivo dopamine levels data are presented as the mean values of six replicates for each sample and the calibration curve was made up with 10 points from 1.5 to 400 ng total with six repeats also for each standard solution.

Ex vivo molecular data (vehicle n = 5; JWH-018 n = 5) are presented as percentage of response in control mice and were analysed by unpaired Student's *t*-tests.

Significance for all tests was assumed at $P < 0.05$. Statistical analyses were performed using GraphPad Prism 6 (GraphPad, Software Inc., San Diego, CA).

2.10 | Nomenclature of targets and ligands

Key protein targets and ligands in this article are hyperlinked to corresponding entries in http://www.guidetopharmacology.org, and are permanently archived in the Concise Guide to PHARMACOLOGY 2021/22 (Alexander, Christopoulos et al., 2021; Alexander, Fabbro, Kelly, Mathie, Peters, Veale, Armstrong, Faccenda, Harding, Pawson, Southan, Davies, Beuve et al., 2021, Alexander, Fabbro, Kelly, Mathie, Peters, Veale, Armstrong, Faccenda, Harding, Pawson, Southan, Davies, Boison et al., 2021; Alexander, Mathie et al., 2021).

3 | RESULTS

To investigate the long-lasting effects of JWH-018 exposure, mice were injected with JWH-018 [6 mg·kg^{-1}·day^{-1} i.p. for seven consecutive days (D1 to D7)], or its vehicle (i.e., control group) or NESS-0327 (1 mg·kg^{-1}) or NESS-0327 (1 mg·kg^{-1}) + JWH-018 (6 mg·kg^{-1}). After 15–16 days of washout (D22-D23), behavioural or biochemical studies were performed (Figure 1).

3.1 | Behavioural experiments

3.1.1 | Motor studies

The group of mice treated with JWH-018 displayed a transient facilitation of spontaneous motor activity in the first 15 min when compared with vehicle- or NESS-0327 (1 mg·kg^{-1})-treated mice [Figure 2a; treatment ($F_{3,\ 864} = 8.782$, $P < 0.05$)]. The pre-treatment with NESS-0327 (1 mg·kg^{-1}) prevented the motor impairment induced by JWH-018 (6 mg·kg^{-1}). In mice treated with JWH-018, motor activation was characterized by an increase in the number of entries into the central [-Table 1; treatment ($F_{3,\ 28} = 10.11$, $P < 0.05$)] and peripheral [Table 1; treatment ($F_{3,\ 28} = 6.746$, $P = 0.0014$)] areas of the open field arena, by longer times of permanence in the central [Table 1; treatment ($F_{3,\ 28} = 28.92$, $P < 0.05$)] with respect to the peripheral [Table 1; treatment ($F_{3,\ 28} = 6.314$, $P < 0.0021$)] area, and by an increase in the number of rotations of animal's body [Table 1; treatment ($F_{3,\ 28} = 24.13$, $P < 0.05$)], while no significant differences in maximum [Table 1; treatment ($F_{3,\ 28} = 2.872$, $P = 0.0541$)] and average speed [Table 1; treatment ($F_{3,\ 28} = 2.467$, $P = 0.0828$)] were found between the groups. In the drag test, the repeated administration of JWH-018 induced an increase in the number of steps performed with the front legs of mice [-Figure 2b; treatment ($F_{3,\ 36} = 9.951$, $P < 0.05$)]. This effect was totally prevented by pre-treatment with NESS-01327 (1 mg·kg^{-1}; Figure 2b). In addition, in the accelerod test, a facilitation on the motor performance was displayed in mice treated with JWH-018 [Figure 2c; treatment ($F_{3,\ 36} = 14.51$, $P < 0.05$)], and this effect was totally prevented by pre-treatment with NESS-01327 (1 mg·kg^{-1}; Figure 2c).

3.1.2 | Novel object recognition test

The group of mice treated with JWH-018 showed a significant impairment in the discrimination of the novel object [Figure 3a; treatment ($F_{3,\ 28} = 29.97$, $P < 0.05$)] and in spatial memory [Figure 3c; treatment

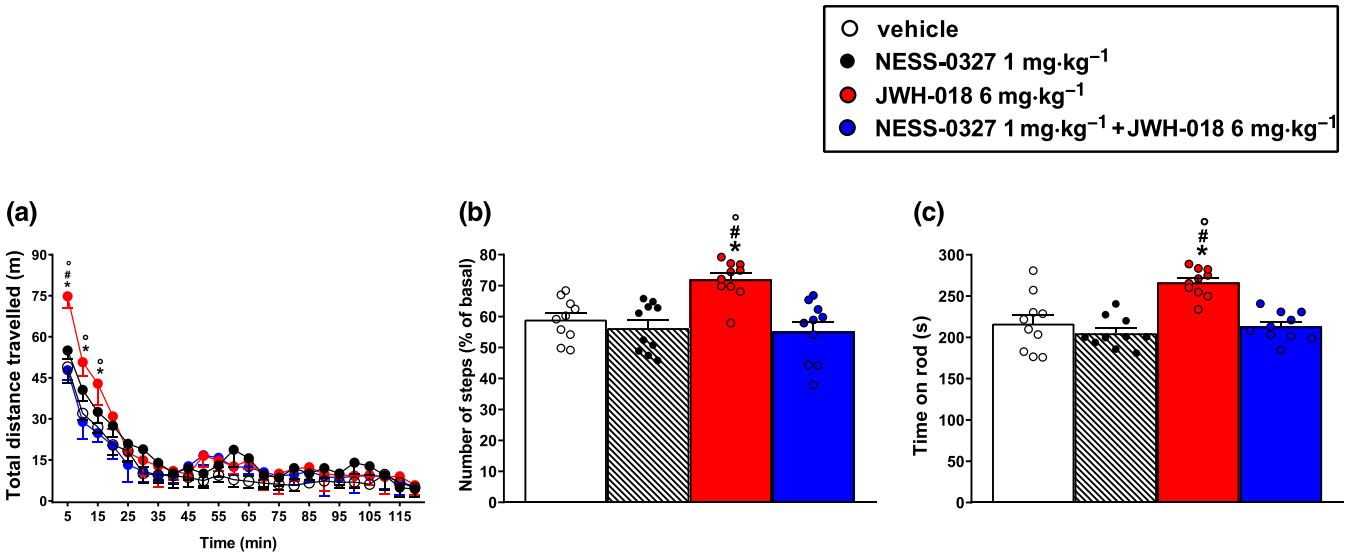

FIGURE 2 Long-term effects of repeated administration of the CB_1 receptor antagonist NESS-0327 (1 mg·kg^{-1}), the synthetic cannabinoid JWH-018 (6 mg·kg^{-1}) or NESS-0327 (1 mg·kg^{-1}) + JWH-018 (6 mg·kg^{-1}) on spontaneous and stimulated motor activity of mice. Motor response of mice on the total distance travelled (panel a), the drag test (panel b) and the accelerod test (panel c) at day 22 (D22). Mice were treated for 7 days (from day 1 to day 7) once a day with JWH-018 (6 mg·kg^{-1}; black) or vehicle (white). Data are expressed (see Section 2) as total distance travelled in metres, number of steps or time on rod in seconds and represent the mean ± SEM of 10 animals for each treatment. Statistical analysis was performed by two-way ANOVA followed by the Bonferroni's test for multiple comparisons in panel (a) and with one-way ANOVA followed by the Bonferroni's test for multiple comparisons in panels (b) and (c). The statistical analysis was performed with Prism software (GraphPad Prism, Boston, USA). *P < 0.05 versus vehicle; $^{\#}P$ < 0.05 versus NESS-0327; °P < 0.05 versus NESS-0327 + JWH-018.

TABLE 1 Long-term effect of repeated administration of the CB_1 receptor- antagonist NESS-0327 (1 mg·kg^{-1}), JWH-018 (6 mg·kg^{-1}) or NESS-0327 (1 mg·kg^{-1}) + JWH-018 (6 mg·kg^{-1}) administration on spontaneous motor activity of mice.

		Vehicle	NESS-0327	JWH-018	NESS-0327 + JWH-018
Central area	Number of entries	26.3 ± 2.6	27.6 ± 3.9	48.9 ± 4.5*	30.1 ± 1.4
	Total time (s)	29.4 ± 2.9	27.5 ± 1.7	69.90 ± 5.9*	28.9 ± 3.6
Peripheral area	Number of entries	26.7 ± 2.8	28.0 ± 4.1	50.3 ± 3.8*	29.1 ± 5.9
	Total time (s)	872.0 ± 1.5	859.4 ± 6.6	838.6 ± 8.4*	866.3 ± 4.3
Rotation of animal's body	Number of rotations	34.4 ± 2.6	30.2 ± 3.9	66.2 ± 3.4*	36.2 ± 7.5
Maximum speed	(m·s^{-1})	0.298 ± 0.006	0.302 ± 0.007	0.312 ± 0.008	0.285 ± 0.005
Average speed	(m·s^{-1})	0.087 ± 0.005	0.079 ± 0.006	0.098 ± 0.004	0.091 ± 0.005

Note: Motor activity measurements of mice on time spent in the central and peripheral area, entries in the central and peripheral area, rotations of animal's body, maximum and average running speed were analysed in the first 15 min. Mice were treated for 7 days (from day 1 to day 7) once a day with the CB_1 receptor- antagonist NESS-0327 (1 mg·kg^{-1}), JWH-018 (6 mg·kg^{-1}), vehicle or NESS-0327 (1 mg·kg^{-1}) + JWH-018 (6 mg·kg^{-1}) and tested at day 22. Data are expressed (see Section 2) as time spent in the central and peripheral area (in seconds), entries in the central and peripheral area (no. of entries), rotations of animal's body (no. of rotations), maximum and average running speed (m·s^{-1}) and represent the mean ± SEM of 10 animals for each treatment. Statistical analysis was performed by one-way ANOVA followed by the Bonferroni's test for multiple comparisons. The statistical analysis was performed with the program Prism software (GraphPad Prism, USA). *P < 0.05, versus vehicle.

($F_{3,\ 28} = 12.45$, $P < 0.05$)] with respect to the groups of mice treated with the vehicle or NESS-0327 (1 mg·kg^{-1}). This effect was totally prevented by pre-treatment with NESS-01327 (1 mg·kg^{-1}; Figure 3a,c). The total object exploration time was significantly reduced in mice treated with JWH-018 in the object memory [Figure 3b; treatment ($F_{3,\ 28} = 15.15$, $P < 0.05$)] and in the spatial memory tests [Figure 3d; treatment ($F_{3,\ 28} = 12.04$, $P < 0.05$)]. The impairment in the total object exploration time induced by JWH-018 (6 mg·kg^{-1}), in object and spatial memory, was totally prevented by pre-treatment with NESS-0327 (1 mg·kg^{-1}; Figure 3b,d).

3.1.3 | Tail suspension and social dominance test

In the tail suspension test, a significant reduction in the immobility time was observed in mice treated with JWH-018 with respect to the groups of mice treated with the vehicle or NESS-0327 (1 mg·kg^{-1}), with an increase of escaping movements and body shaking in mice [Figure 4a; treatment ($F_{3,\ 28} = 14.40$, $P < 0.05$)]. This effect was totally prevented by pre-treatment with NESS-01327 (1 mg·kg^{-1}; Figure 4a). In the social dominance test, the group of mice treated with JWH-018 abandoned the tube in

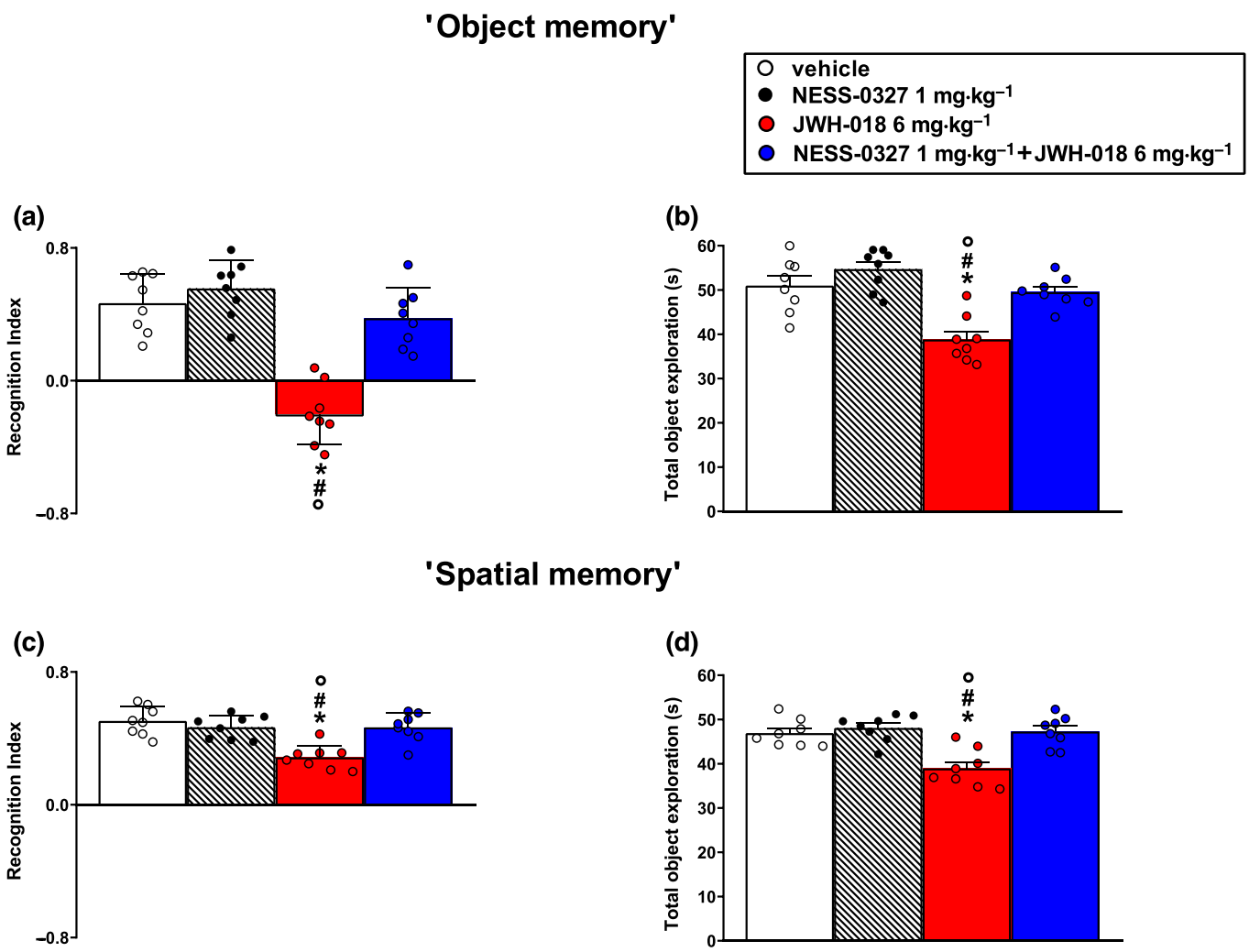

FIGURE 3 Long-term effects of repeated administration of the CB_1 receptor antagonist NESS-0327 (1 mg·kg^{-1}), the synthetic cannabinoid JWH-018 (6 mg·kg^{-1}) or NESS-0327 (1 mg·kg^{-1}) + JWH-018 (6 mg·kg^{-1}) on recognition and spatial memory in mice. Response of mice in the novel 'object' (panels a and b) and 'spatial' (panels c and d) memory tests at day 22 (D22). The recognition index of mice in the 'novel object' test is reported in panel (a), and the total object exploration in panel (b). The recognition index of mice in the 'spatial' test is reported in panel (c), and the total object exploration in panel (d). Mice were treated for 7 days (from day 1 to day 7) once a day with JWH-018 (6 mg·kg^{-1}; black) or vehicle (white). Data are expressed as recognition index (panels a and c; see Section 2) or as total object exploration in seconds (panels b and d) and represent the mean ± SEM of eight animals for each treatment. Statistical analysis was performed by one-way ANOVA followed by the Bonferroni's test for multiple comparisons. The statistical analysis was performed with the program Prism software (GraphPad Prism, USA). *P < 0.05 versus vehicle; $^{\#}P$ < 0.05 versus NESS-0327; $^{\circ}P$ < 0.05 versus NESS-0327 + JWH-018.

greater percentage with respect to the vehicle or NESS-0327 (1 mg·kg^{-1}) groups, highlighting more defeats at D22 [Figure 4b; treatment ($F_{3,\ 28} = 35.56$, $P < 0.05$)].

3.1.4 | Startle amplitude and prepulse inhibition test

Administration of JWH-018 inhibited, compared with the groups of mice treated with vehicle or NESS-0327 1 mg·kg^{-1}, both startle amplitude [Figure 5a; treatment ($F_{3,\ 32} = 17.46$, $P < 0.05$)] and prepulse inhibition test (Figure 5b) in mice at D23. Indeed, statistical analysis detected a significant decrease of prepulse intensity with 68 dB (∼19%; treatment: $F_{3,\ 32} = 9.242$, $P < 0.05$), 75 dB [∼24%; treatment ($F_{3,\ 32} = 39.97$, $P < 0.05$)] and 85 dB [∼15%; treatment ($F_{3,\ 32} = 12.03$, $P < 0.05$)], respectively. The effects induced by JWH-018 (6 mg·kg^{-1}) in the prepulse inhibition test were totally prevented by pre-treatment with NESS-0327 (1 mg·kg^{-1}; Figure 5a,b).

3.2 | In vivo microdialysis

Basal extracellular striatal glutamate levels, evaluated as the mean of three stable dialysates, were similar in both JWH-018- and vehicle-treated mice (Figure 6a). A 10-min pulse of high K^+ (50 mM) solution significantly increased glutamate efflux in both groups of animals. However, the K^+-evoked glutamate efflux from the striatum of mice treated with JWH-018 was significantly higher

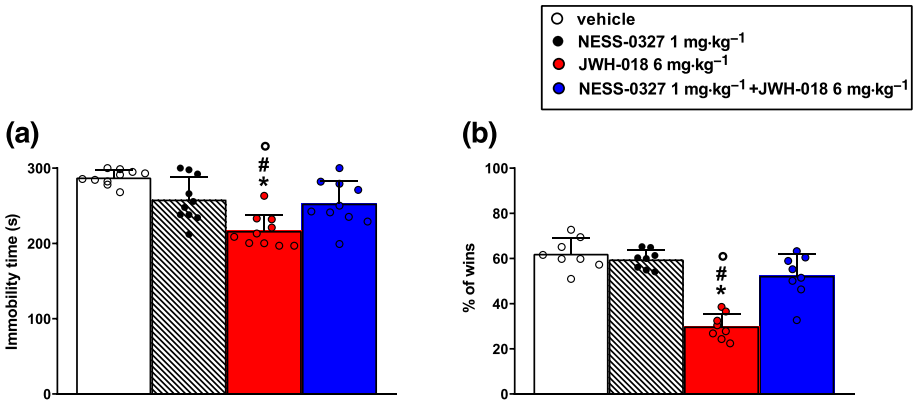

FIGURE 4 Long-term effect of repeated administration of the CB_1 receptor antagonist NESS-0327 (1 mg·kg^{-1}), the synthetic cannabinoid JWH-018 (6 mg·kg^{-1}) or NESS-0327 (1 mg·kg^{-1}) + JWH-018 (6 mg·kg^{-1}) on immobility time in the tail suspension test and in the social dominance test in mice. Response of mice in the tail suspension (panel a) and in the social dominance (panel b) test at day 22 (D22). Mice were treated for 7 days (from day 1 to day 7) once a day with JWH-018 (6 mg·kg^{-1}; black) or vehicle (white). Data are expressed as immobility time in seconds (s; panel a) and % of wins (panel b) and represent the mean ± SEM of 10 (panel a) or 8 (panel b) animals for each treatment. Statistical analysis was performed by one-way ANOVA followed by the Bonferroni's test for multiple comparisons. The statistical analysis was performed with the program prism software (GraphPad Prism, USA). *P < 0.05 versus vehicle; $^{\#}P$ < 0.05 versus NESS-0327; $^{\circ}P$ < 0.05 versus NESS-0327 + JWH-018.

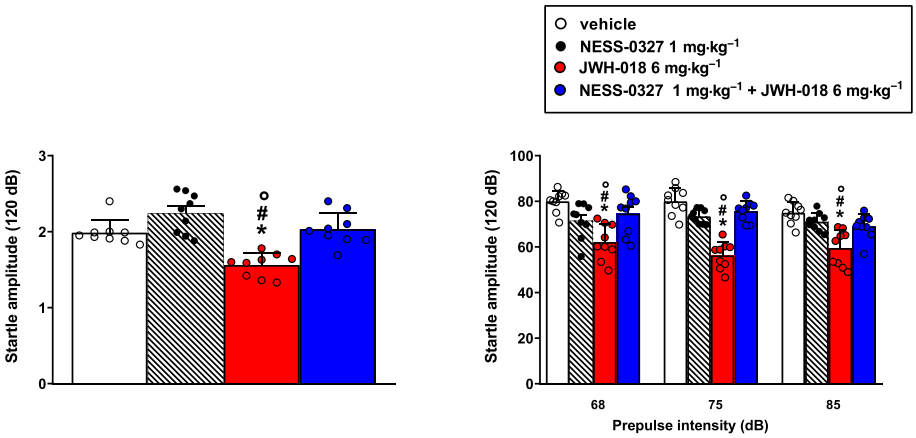

FIGURE 5 Long-term effect of repeated administration of the CB_1 receptor antagonist NESS-0327 (1 mg·kg^{-1}), the synthetic cannabinoid JWH-018 (6 mg·kg^{-1}) or NESS-0327 (1 mg·kg^{-1}) + JWH-018 (6 mg·kg^{-1}) in the startle amplitude and prepulse inhibition test in mice. Response of mice in the startle amplitude (panel a) and prepulse inhibition (panel b) test in mice at day 23 (D23). Mice were treated for 7 days (from day 1 to day 7) once a day with JWH-018 (6 mg·kg^{-1}; black) or vehicle (white). Effects on pre-pulse inhibition (PPI) are shown for the three prepulse intensities (68, 75 and 85 dB). Data are expressed as startle amplitude in decibel (dB; panel a) and as % of prepulse inhibition (see Section 2; panel b) and represent the mean ± SEM of nine animals for each treatment. Statistical analysis was performed by one-way ANOVA followed by the Bonferroni's test for multiple comparisons. The statistical analysis was performed with the program Prism software (GraphPad Prism, USA). *P < 0.05 versus vehicle; $^{\#}P$ < 0.05 versus NESS-0327; $^{\circ}P$ < 0.05 versus NESS-0327 + JWH-018.

($t = 2.404$, $df = 16$, $P = 0.0287$) than the enhancement observed in vehicle-treated animals (Figure 6b). Finally, after a 5 min disturbing period, an increase, although not significant, in basal extracellular striatal glutamate levels was observed in mice treated with JWH-018, but not in vehicle-treated animals (Figure 6c).

3.3 | Ex vivo striatal dopamine content

The group of mice treated with JWH-018 showed a significant increase of striatal dopamine content [Figure 7; treatment ($F_{3,\ 28} = 12.60$, $P < 0.05$)] with respect to the groups of mice treated with the vehicle or NESS-0327 (1 mg·kg^{-1}). This effect was totally prevented by pre-treatment with NESS-01327 (1 mg·kg^{-1}; Figure 7).

3.4 | In vitro electrophysiological studies

3.4.1 | Effects on synaptic excitatory transmission and on plasticity in the CA1 hippocampal area

Once a stable synaptic response had been obtained, an SRC was obtained as previously stated (see materials and methods). Figure 8b

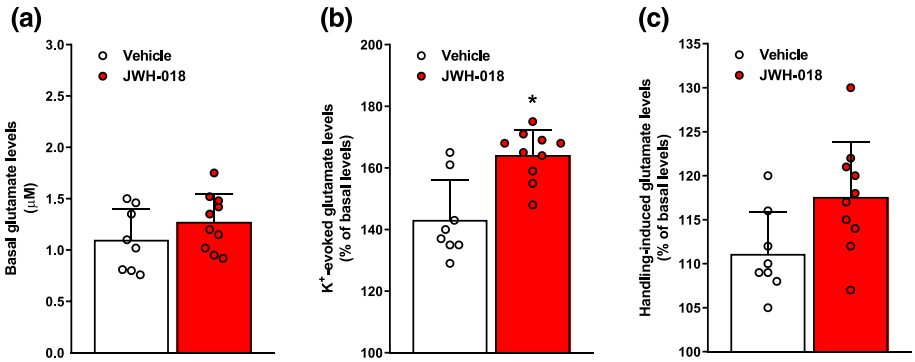

FIGURE 6 Long-term effect of repeated administration of the synthetic cannabinoid JWH-018 on basal and evoked extracellular glutamate levels in mouse striatum. Mice were treated for 7 days (from day 1 to day 7) once a day with JWH-018 (6 mg·kg^{-1}; red) or vehicle (white); basal (panel a), K^+-evoked (panel b) and disturbing (panel c) evoked striatal extracellular levels were measure by means of microdialysis in mice at day 23 (D23; i.e., 16 days after the last drug administration). For further details, see Section 2. Data are the mean ± SEM; n = 8–10 per group. Statistical analysis was performed by Student's *t*-test, using the program Prism software (GraphPad Prism, USA). *P < 0.05 significantly different from the respective vehicle group.

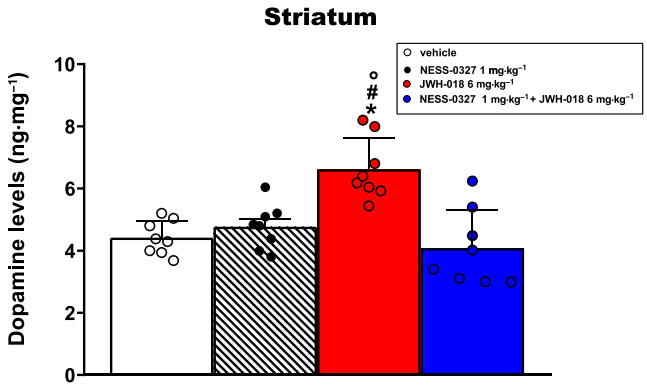

FIGURE 7 Long-term effect of repeated administration of the synthetic cannabinoid JWH-018 on dopamine levels in mice striatum. Mice were treated for 7 days (from day 1 to day 7) once a day with vehicle, the CB_1 receptor antagonist NESS-0327 (1 mg·kg^{-1}), JWH-018 (6 mg·kg^{-1}) or NESS-0327 (1 mg·kg^{-1}) + JWH-018 (6 mg·kg^{-1}). Basal striatal extracellular levels were measure by UPLC in mice at day 23 (D23; i.e., 16 days after the last drugs). For further details, Section 2. Data are the mean ± SEM; n = 8 per group. Statistical analysis was performed by one-way ANOVA followed by the Bonferroni's test for multiple comparisons. The statistical analysis was performed with the program Prism software (GraphPad Prism, USA). *P < 0.05 versus vehicle; $^{\#}P$ < 0.05 versus NESS-0327; $^{\circ}P$ < 0.05 versus NESS-0327 + JWH-018.

compares the data fittings with the resulting normalized sigmoid curve from which the EC_{50} values were extrapolated (Figure 8c). Statistical comparison of the fits indicated a significant difference between the two curves (P < 0.05). The EC_{50} parameters were also different (1.75 ± 0.07 vs. 1.6 ± 0.07, vehicle vs. JWH-018, n = 6 both groups, P < 0.05). These two pieces of evidence suggest a long-term effect of JWH-018 treatment, resulting in increased hippocampal network excitability. The EC_{50} was then used as a reference for stimulation intensity for the TB5-protocol for LTP induction. Figure 8d compares representative fEPSP recordings, superimposed from vehicle-treated (above in the panel) and JWH-018-treated animal (below) in control and after TB5 at steady slope amplitude. It is impressive how JWH-018 pretreatment completely blocks the induced potentiation visible in the control experiment. Figure 8e shows the superimposed time-course of normalized average experimental points of LTP test experiments in the two groups. TB5 induced a long lasting and stable potentiation in vehicle treated mice, while JWH-018 significantly weakened this development, impairing the formation of any consistent stable early and late LTP, and showing a significative statistical difference (2.22 ± 0.7 vs. 1.12 ± 0.6, fold normalized fEPSP increase vs. fEPSP slope baseline; P < 0.05). Figure 8f summarizes peak values seen in the previous panel, taken at 40 min after TB5, at steady fEPSP slope for the two groups, showing a significative statistical difference (122 ± 6% vs. 12 ± 7%, vehicle vs. JWH-018 pretreated; t = 12.16; df = 10; P < 0.05, n = 6 both groups). In both groups, the TB10 saturating test (see methods) was unable to induce any further potentiation, confirming the strong LTP-inhibition from JWH-018 treatment (data not shown).

To verify if the hippocampal synaptic pathway (and excitability, by consequence) was modified between vehicle and JWH-018 D23 -treated mice, stimulation voltage necessary to evoke the 50% of maximal fEPSP was extrapolated from SRC curves (Figure 8b). Results were normalized as stimulation fold increase for comparison (1.77 ± 0.4 vs. 1.58 ± 0.7, fold increase, vehicle vs. JWH-018, n = 6 per group). These data show a moderate, but nonsignificant, difference between the two groups, with JWH-018 group being slightly more excitable. For TB5 stimulation protocol, the stimulation intensity calculated from SRC was used (see Section 2) to induce synaptic potentiation. Figure 8c shows superimposed representative recordings, comparing fEPSP traces from vehicle and JWH-018 D23 mice, before and after TB5. Normalized average experimental points of the LTP test, comparing fEPSPs slope from two groups are shown in

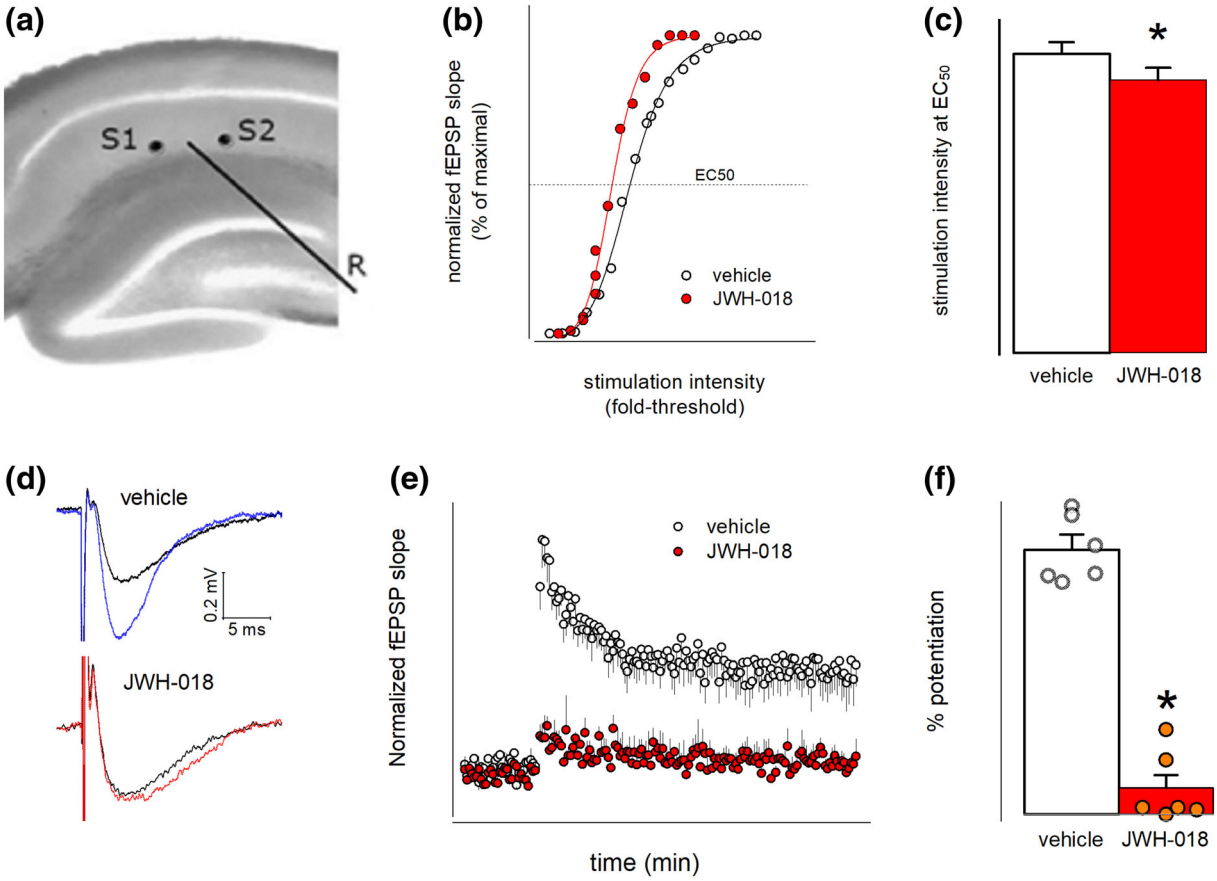

FIGURE 8 Long-term effect of repeated administration of the synthetic cannabinoid JWH-018 on LTP in mice hippocampal slices. The mice used in this study were killed on day 23, which was 16 days after the last administration of either vehicle or JWH-018. In all panels n = 6, both groups; hollow symbol: vehicle; red symbol: JWH-018 at D23. **P*-value < 0.05. (a) Scheme for the arrangement of stimulating and recording electrodes on a hippocampal slice. The stimulating electrodes (S1 and S2) were placed in the stratum radiatum at opposite sites relative to the recording electrode (R) located in the dendritic region of the CA1 area (see Section 2 for more details). (b) Stimulus\response (SRC)-sigmoid curve extrapolated from stimulus\response protocol data (see Section 2). (c) Histogram comparing the EC_{50} values ± SD, extrapolated from curves in panel (b). (d) Two superimposed representative field excitatory postsynaptic potential (fEPSP) curves before (black) and after theta burst (TB5) stimulation, recorded from vehicle (top, blue trace) and JWH-018 D23 (bottom, red trace) treated mice, at steady state LTP. (e) Time course of recorded fEPSP slope modification upon induced LTP after TB5 tetanic stimulation (at time 0). Time values ± SEM were averaged then normalized with pre-TB5 values. (f) Histogram summarizing the differences (as % of potentiation) as steady effect on fEPSP of TB5 (at stable LTP), versus pre-TB5 baseline values ± SEM.

Figure 8d, plotted as a time course. Clearly, with different potentiating effect of TB5 exemplified in Figure 8c, comparison between the LTP induced in the two groups, shows how the pretreatment with JWH-018 reduced the development of early and late LTP (normalized fEPSP increase vs. fEPSP slope baseline, 2.22 ± 0.7-fold vs. 1.12 ± 0.6, vehicle vs. JWH-018 treated groups), impairing the formation of a stable potentiation. In all tests, subsequently to stable fEPSP after TB5, a further test using the TB10 protocol was applied and resulting values used to calculate potentiation as indicated in the statistical methods. In all slices this saturating procedure was unable to induce any further visible potentiation. Figure 8e compares LTP values as % potentiation after TB5, at steady fEPSP slope, showing a significant statistical difference between the two treatments (122 ± 6% vs. 12 ± 7%, vehicle vs. JWH-018 pretreated, $P < 0.05$, n = 6 per group).

3.5 | Ex vivo biochemical studies

3.5.1 | BDNF expression and signalling in the mouse hippocampus

Figure 9 shows that the mature form of BDNF (mBDNF) was significantly reduced in the hippocampus of JWH-018-treated animals (mBDNF: −42%, $t = 3.492$, $df = 8$, $P = 0.0082$; panel a), compared with vehicle-treated animals. Interestingly, such a reduction was observed also in BDNF-related intracellular signalling. In fact, the expression and phosphorylation of **trkB**, that is, the high affinity BDNF receptor, is significantly reduced in mice exposed to repeated injections of JWH-018 (pTrkB: −37%, $t = 2.599$, $df = 8$, $P = 0.0316$; TrkB: −34%, $t = 3.164$, $df = 8$, $P = 0.0133$; panel b). In line with the reduction of BDNF–trkB mediated signalling, the BDNF-dependent

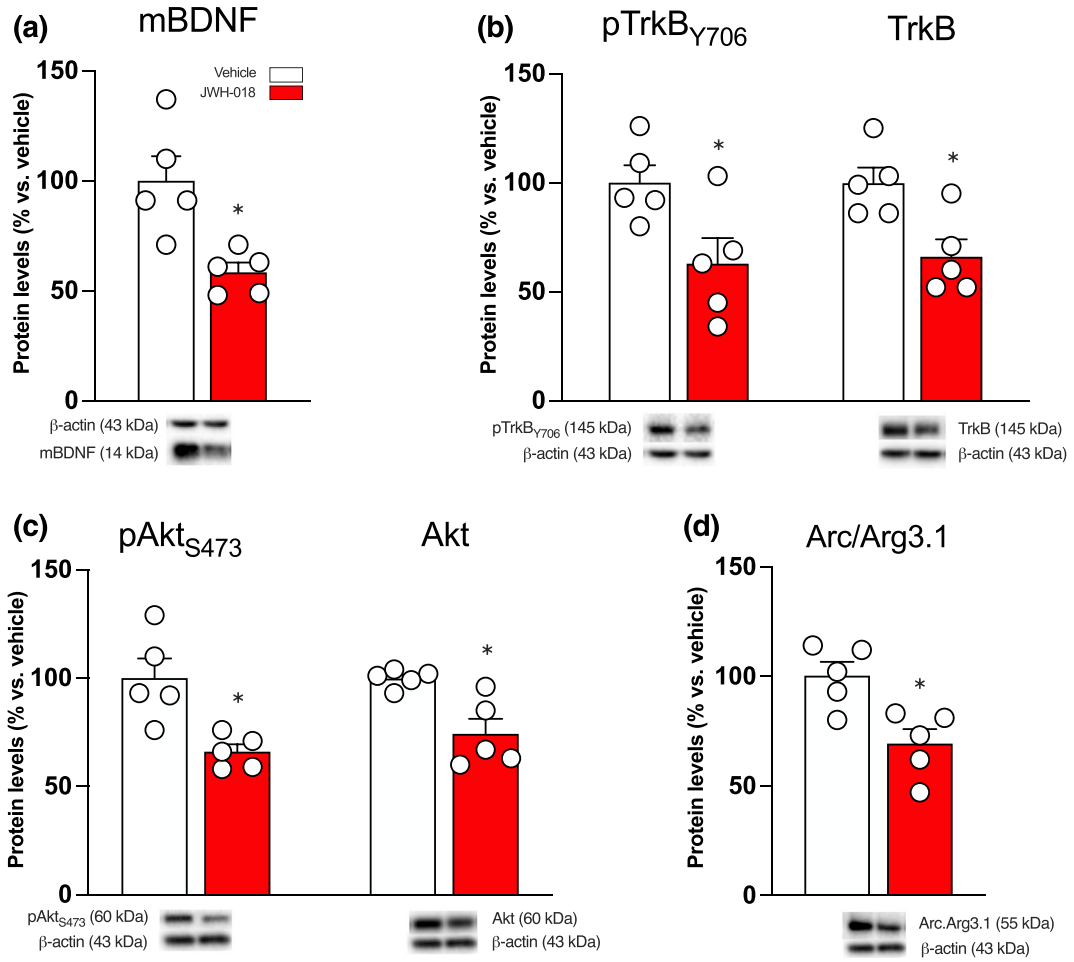

FIGURE 9 Long-term effect of repeated administration of the synthetic cannabinoid JWH-018 on BDNF and its intracellular signalling pathway expression and activation as well as on the expression of arc/Arg3.1 in the hippocampus. (a) mBDNF protein levels in the whole homogenate of the hippocampus of vehicle and-JWH018-treated mice. (b) the phosphorylation in Tyr706 (left side) and the total form (right side) of the trkB receptor. (c) the phosphorylation in Ser473 (left side) and the total form (right side) of the Akt kinase, one of the major intracellular signals activated by BDNF. (d) the expression of arc/Arg3.1 in the homogenate of hippocampus. Mice were killed 15 days after the last drug exposure. Below each graph, representative immunoblots are shown for mBDNF (14 kDa), pTrkB Y706 (145 kDa), TrkB (145 kDa), pAkt S473 (60 kDa), Akt (60 kDa) and β-actin (43 kDa) proteins in the homogenate of mouse hippocampus. Each set of proteins was run in the same WB assay, thus only one band of β-actin is represented. Results are expressed as percentages of vehicle-treated mice. Histograms represent the mean ± SEM of five mice per group. *$P < 0.05$ versus vehicle-treated mice (unpaired Student's *t*-test).

Akt pathway was also reduced, both in terms of phosphorylation and expression (pAkt S473: −34%, $t = 3.557$, $df = 8$, $P = 0.0074$; Akt: −26%, $t = 3.308$, $df = 8$, $P = 0.0107$; panel c). Finally, a reduced expression of hippocampal Arc/Arg3.1 (−31%, $t = 3.641$, $df = 8$, $P = 0.0066$; panel d) was observed in JWH-018 treated mice, when compared with vehicle-treated animals.

3.5.2 | Glutamate NMDA receptor and PSD95 expression in the mouse striatum and hippocampus

Figure 10 shows that the expression of the integral protein of the glutamate synaptic PSD95 was significantly reduced specifically in the crude synaptosomal fraction of the striatum of JWH-018-treated mice (crude synaptosomal fraction: −21, $t = 3.314$, $df = 8$, $P = 0.016$; panel g). The analysis of the expression of the NMDA receptor subunits revealed that the expression of the main subunit GluN1 as well as the accessory subunits GluN2A and GluN2B were reduced in the crude synaptosomal fraction (GluN1: −19%, $t = 3.006$, $df = 8$, $P = 0.0169$, panel a; GluN2A: −20%, $t = 4.289$, $df = 8$, $P = 0.0027$, panel c; GluN2B: −26%, $t = 3.825$, $df = 8$, $P = 0.0051$, panel e) and not in the homogenate (GluN1: +6%, $t = 1.343$, $df = 8$, $P = 0.216$, panel a; GluN2A: +12%, $t = 1.522$, $df = 8$, $P = 0.1664$, panel c; GluN2B: +14%, $t = 1.847$, $df = 8$, $P = 0.1019$, panel e) of the striatum of JWH-018-treated mice.

As shown in striatum, we found a similar reduction of PSD95 in the crude synaptosomal fraction of the hippocampus of JWH-018-treated mice (−24%, $t = 3.314$, $df = 8$, $P = 0.0106$; panel h). In

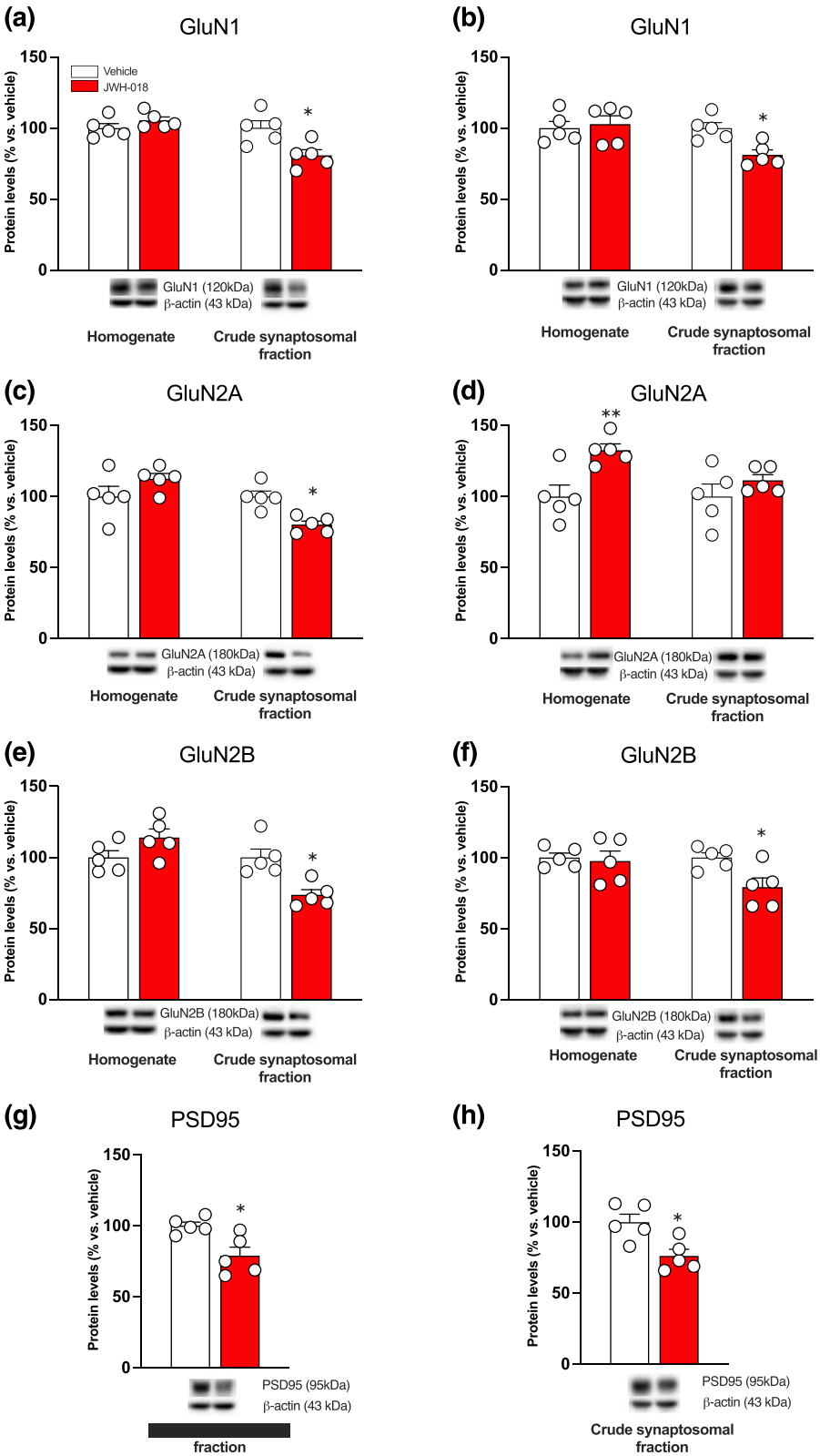

FIGURE 10 Long-term effects of repeated administration of the synthetic cannabinoid JWH-018 on the NMDA receptor subunits and on PSD95 expression in the striatum and the hippocampus. Mice were killed 15 days after the last exposure to JWH018. Protein levels of GluN1 (a), GluN2A (c) and GluN2B (e) were measured in the homogenate (left) and in the crude synaptosomal fraction (right) of the striatum. (g) the expression of PSD95 in the crude synaptosomal fraction of the striatum. Protein levels of GluN1 (b), GluN2A (d) and GluN2B (f) were measured in the homogenate (left) and in the crude synaptosomal fraction (right) of the hippocampus. (h) the expression of PSD95 in the crude synaptosomal fraction of the hippocampus. Below each graph, representative immunoblots are shown for GluN2A (180 kDa), GluN2B (180 kDa), GluN1 (120 kDa) and PSD95 (95 kDa) proteins in the mouse striatum. Each set of proteins was run in the same WB assay, thus only one band of β-actin is represented. Results are expressed as percentages of vehicle-treated mice. Histograms represent the mean ± SEM of five mice per group. $^*P < 0.05$ versus vehicle-treated mice (unpaired Student's *t*-test).

line with the results observed in striatum, we found a reduction of GluN1 and GluN2B in the crude synaptosomal fraction (GluN1: −19%, $t = 3.581$, $df = 8$, $P = 0.0072$, panel b; GluN2B: −21%, $t = 2.844$, $df = 8$, $P = 0.0217$, panel f), but not in the homogenate (GluN1: +3%, $t = 0.3684$, $df = 8$, $P = 0.7221$, panel b; GluN2B: −2%, $t = 0.3021$, $df = 8$, $P = 0.7703$, panel f). At variance from striatum,

we found increased expression of GluN2A in the homogenate (GluN2A: +32%, $t = 3.538$, $df = 8$, $P = 0.0076$, panel d), and no significant effects in the crude synaptosomal fraction (GluN2A: +11%, $t = 1.172$, $df = 8$, $P = 0.2749$, panel d).

3.5.3 | Protein levels of the main synthetic and degrading enzymes of anandamide (AEA) and 2-arachidonoylglycerol (2-AG)

Figure 11 represents the effect of repeated JWH-018 treatment on protein levels of the main synthetic and degrading enzymes of AEA (NAPE-PLD and FAAH, respectively) and 2-AG (DAGLα and MAGL, respectively) in the striatum (a) and hippocampus (b). In the striatum, JWH-018 administration significantly increased the expression of FAAH (+45.7%; $t = 2.362$, $df = 8$, $P = 0.0458$) and MAGL (+73.6%; $t = 2.537$, $df = 8$, $P = 0.0349$) without affecting protein levels of the synthetic enzymes NAPE-PLD ($t = 0.2894$, $df = 8$, $P = 0.7796$) and DAGLα ($t = 1.317$, $df = 8$, $P = 0.2244$). In contrast, in the hippocampus no changes in protein levels of NAPE-PLD ($t = 1.844$, $df = 8$, $P = 0.1025$), DAGLα ($t = 0.3117$, $df = 8$, $P = 0.7632$), FAAH ($t = 0.9912$, $df = 8$, $P = 0.3506$) and MAGL ($t = 1.215$, $df = 8$, $P = 0.2591$) were observed.

3.5.4 | CB_1 receptor density in the striatum and hippocampus

Figure 12 represents the effects of repeated JWH-018 treatment on CB_1 receptor density as measured by means of autoradiographic binding assays in the striatum (a) and hippocampus (b). No changes in CB_1 receptor density were observed in the striatum ($t = 1.389$, $df = 9$, $P = 0.1981$). In contrast, autoradiographic binding studies revealed a significant reduction of CB_1 receptor density by about 23% ($t = 3.473$, $df = 9$, $P = 0.0070$) in the hippocampus of JWH-018-treated mice compared with controls.

3.5.5 | 2-AG and AEA levels in the striatum

To elucidate the impact of the alterations in protein levels of the main endocannabinoid enzymes observed in the striatum, we evaluated in this brain region the levels of AEA and 2-AG. As reported in Figure 13, a significant and remarkable increase in AEA levels was present in the striatum of JWH-018-treated mice compared with controls (5.4 vs. 0.5 pg·μg^{-1} proteins, respectively; $t = 54.84$, $df = 9$, $P < 0.05$), while a more modest, but still significant, elevation was

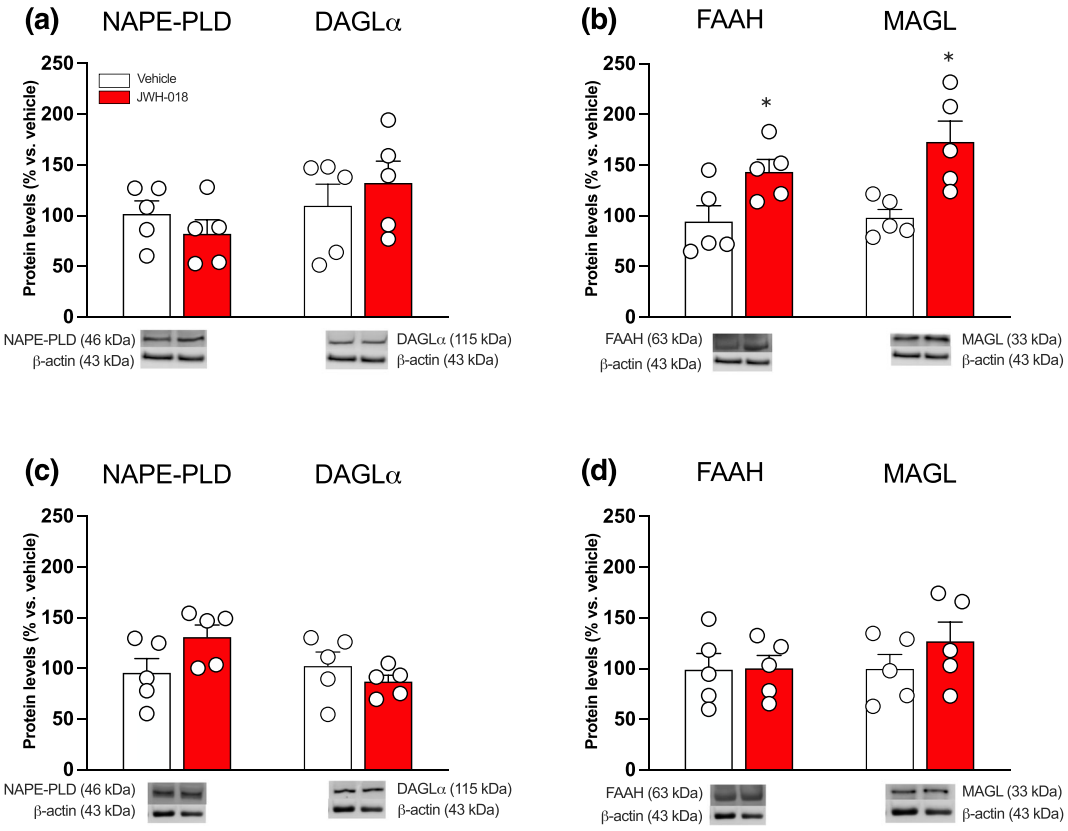

FIGURE 11 Long-term effect of repeated JWH-018 administration on protein levels of the main endocannabinoid synthetic (NAPE-PLD and DAGLα) and degrading (FAAH and MAGL) enzymes as measured by Western blot analyses of total protein lysates obtained from the striatum (panel a) and hippocampus (panel b). Each set of proteins was run in the same WB assay, thus only one band of β-actin is represented. Data represent mean ± SEM of five vehicle- and five JWH-018-treated mice with each experimental value from three replicates. *$P < 0.05$ versus vehicle (Student's *t*-test).

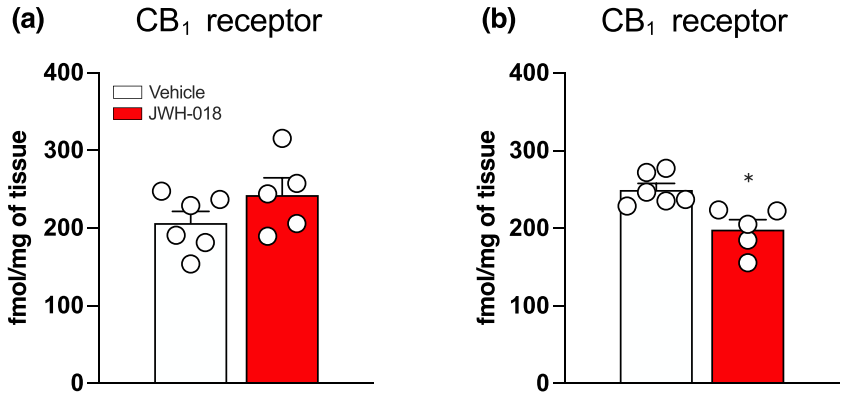

FIGURE 12 Long-term effect of repeated administration of the synthetic cannabinoid JWH-018 on CB_1 receptor density in the striatum (a) and hippocampus (b) as measured by means of autoradiographic binding assays. Data represent mean ± SEM of 6 vehicle- and 5 JWH-018-treated mice. *$P < 0.05$ versus vehicle (Student's *t*-test).

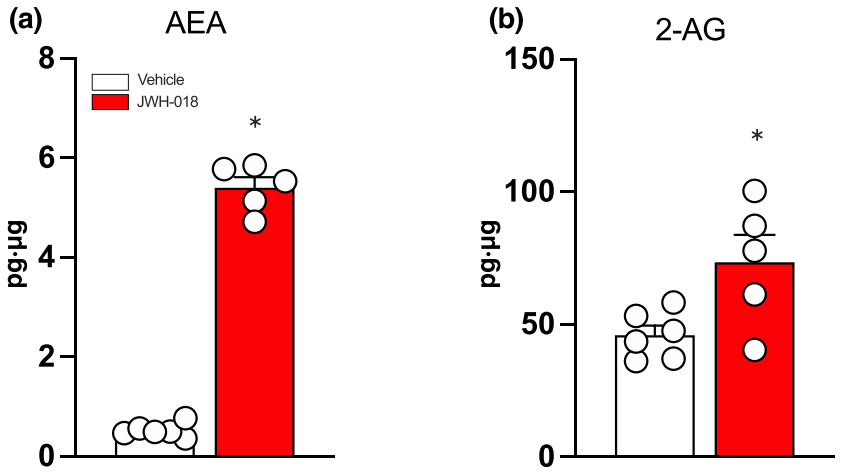

FIGURE 13 Long-term effect of repeated administration of the synthetic cannabinoid JWH-018 on endocannabinoid (AEA and 2-AG) contents in the striatum. Data represent mean ± SEM of six vehicle- and five JWH-018-treated mice. *$P < 0.05$ versus vehicle (Student's *t*-test).

observed in 2-AG (73.4 vs. 45.9 $pg{\cdot}\mu g^{-1}$ proteins, respectively; $t = 6.096$, $df = 9$, $P = 0.05$).

4 | DISCUSSION

The present findings show that repeated exposure to JWH-018 alters neuroplasticity via electrophysiological, neurochemical, and molecular changes in mice together with social and cognitive deficits. These findings are indicative of the development of psychotic-like symptoms adding further concern about the detrimental effects of the abuse of this drug in humans.

4.1 | Behavioural and electrophysiological effects of repeated exposure to the synthetic cannabinoid JWH-018 in mice

Analysis of locomotor activity revealed that repeated exposure to JWH-018 causes a transient facilitation of spontaneous motor activity, an increase of body rotation behaviour and time spent in the centre of the arena, reflecting a moderate psychomotor agitation as we previously observed in mice acutely treated with a low dose of JWH-018 (Ossato et al., 2017). This effect was totally prevented by pre-treatment with the CB_1 antagonist NESS-0327, revealing the involvement of CB_1 receptors in motor activity of mice as previously reported with other CB_1 antagonists (Bilel et al., 2019; Canazza et al., 2016; Corli et al., 2022). Noteworthy, we evaluated the activity of the four groups of mice before treatment (habituation) and we found that there were no differences between the different groups of mice: (vehicle), NESS-0327 (1 $mg{\cdot}kg^{-1}$), JWH-018 (6 $mg{\cdot}kg^{-1}$), (NESS-0327 + JWH-018). This suggests that the effect was induced by JWH-018 treatment and not by the novelty of the environment. Interestingly, the data obtained in the tail suspension test revealed a significant reduction of the immobility time in animals repeatedly treated with JWH-018. The analysis of mouse behaviour in the tail suspension test revealed escaping movements with body shaking in most of the animals that possibly reflects the psychomotor agitation of mice in response to the tail suspension test. Beyond the behavioural impairments shown above, we have also investigated social dominance in JWH-018-treated mice, a measure of social withdrawal, proposed as a sign of negative symptoms in animal models of schizophrenia (Powell & Miyakawa, 2006). By employing the social dominance tube test, we found an increase of subordinated responses in JWH-018-treated mice indicating that vehicle-treated mice were more dominant than mice exposed to JWH-018. We are, however, aware that other experiments will be needed to establish if the defects in social interaction herein shown extend to other

social behaviours such as, for instance, aggression. These impairments were blocked by pre-treatment with the CB_1 antagonist NESS-0327, which reveals that these effects were triggered by the activation of CB_1 receptors even after a long period of washout from the drug.

We also found that repeated exposure to JWH-018 caused a decrease in PPI of the acoustic startle reflex, an operational measure of the sensory gating that is compromised in schizophrenic individuals (Geyer & Braff, 1987; Javitt & Zukin, 1991). A disruption of the PPI after a single administration of JWH-018 or its synthetic halogenated derivatives (JWH-018-Cl, JWH-018-Br) has been demonstrated in a previous study (Bilel et al., 2020), in line with the well-known ability of cannabinoids to alter information processing and sensory disturbances that may be responsible of their psychotic effects in humans (Celofiga et al., 2014; Every-Palmer, 2010, 2011). Interestingly, the sensorimotor gating deficits caused by repeated administration of JWH-018 are long-lasting, being still evident 2 weeks after drug interruption. This is in apparent contrast with a similar recent study, in which no significant effects on PPI were observed at both 24 h and 7 days after the last drug administration (Pintori et al., 2021). The different drug dose (0.25 $mg \cdot kg^{-1}$ vs. 6 $mg \cdot kg^{-1}$), specie of rodents (rats vs. mice) and duration of drug withdrawal used in the two studies could, however, contribute to explain this discrepancy. Moreover, pre-treatment with the CB_1 antagonist NESS-0327 prevented the acoustic alterations observed in mice in the PPI test after the repeated exposure to JWH-018. This result confirms the involvement of the CB_1 receptor in the sensory-gating alterations caused by CB_1-agonists (Bilel et al., 2019; Corli et al., 2022).

We then investigated the effect of long-term withdrawal from repeated JWH-018 exposure on cognition. We demonstrated that JWH-018-treated mice exhibit impaired recognition memory 15 days after drug discontinuation, an effect that was not related to an increase in total object exploration time. Because the novel object recognition (NOR) test is considered a model of short-term memory function (Everts & Koolhaas, 1997), these results suggest that the treatment with JWH-018 induces a long-lasting deficit in short-term information processing. Interestingly, spatial working memory was impaired as well in JWH-018-treated mice, suggesting that long-term withdrawal from JWH-018 has a wide impact on cognition, causing behavioural alterations normally found in schizophrenic patients (Zhang et al., 2012). Our in vitro electrophysiological analysis in brain slices of mice treated with JWH-018 revealed an impairment in LTP. Previous studies revealed that a single JWH-018 administration induced an impairment in short- (2 h) and long-term (24 h) working memory in mice (Barbieri et al., 2016; Barbieri et al., 2022; Li et al., 2019), in line with preclinical studies demonstrating amnesic properties of either natural or SCBs. These alterations have been associated with CB_1 receptor activation and with the ability of the drug to disrupt hippocampal LTP (Barbieri et al., 2016; Barbieri et al., 2022; Hoffman et al., 2017), although treatment with JWH-018 does not substantially modify the synaptic excitability.

4.2 | Homeostasis of the glutamate synapse

In search for neuroplastic changes that could contribute to explain, at least partially, the dysfunctional behaviour of JWH-018-treated mice, we investigated the homeostasis of the glutamate synapse in these mice, focusing on glutamate striatal levels, as well as NMDA receptor and PSD95 expression.

4.2.1 | Effect of repeated exposure to JWH-018 on striatal glutamate levels

While no significant changes were observed in spontaneous basal extracellular striatal glutamate levels, a significant increase in K^+-evoked glutamate efflux and an increase (although not significant) in basal extracellular striatal glutamate levels after a 5 min disturbing period (i.e., generating a noise on top of the grid of the cage using a spatula) were observed 15 days after drug discontinuation, suggesting that the drug preferentially interfered with phasic neurotransmitter release mechanisms.

An increase in glutamate levels has been generally linked to an improvement in neuroplasticity and cognitive tasks and in this context, the present findings are in apparent contrast with the documented JWH-018-induced decrease in plasticity and cognitive impairment. However, it has also been demonstrated that THC elicits subjective and cognitive alterations via increased striatal dopaminergic activity and loss of cortico-striatal connectivity, which is associated with an increase in striatal glutamate and impairment in neurocognitive function (Mason et al., 2019). Thus, it seems likely that these neurochemical alterations could also underlie the JWH-018-induced cognitive-deficit observed in the present study. This hypothesis is supported by the increased striatal dopamine content observed in mice treated with JWH-018 (see below).

4.2.2 | Effect of repeated exposure to JWH-018 on the expression of the different subunits of NMDA receptor and on PSD95

At the molecular level, we first investigated the levels of the NMDA receptor, which is known to be altered in schizophrenic patients (Errico et al., 2013) and animal models of the disease (Konradi & Heckers, 2003; Oka et al., 2020; Wu et al., 2021). In striatum, we found that the expression of the three main subunits of the NMDA receptor, that is, the GluN1, GluN2A and GluN2B, are reduced in the crude striatal synaptosomal fraction, but not in the whole homogenate. In hippocampus, we observed a similar situation, with GluN1 and GluN2B subunit expression reduced only in the crude synaptosomal fraction, whereas the level of GluN2A subunit was significantly enhanced in the whole homogenate and unchanged in the crude synaptosomal fraction. With the exception of the GluN2A subunit, these findings suggest that repeated exposure of JWH-018 does not cause any effect on NMDA receptor subunit translation

but, rather, on their localization at synaptic level. This is strengthened by the evidence of the reduced expression of PSD95, a scaffolding protein essential for NMDA receptor membrane trafficking and signalling (Pérez-Otaño & Ehlers, 2004), confirming the possibility that NMDA receptor membrane retention is impaired following repeated exposure to JWH-018. Of note, because PSD95 is considered to be an index of integrity and stability of excitatory synapses (El-Husseini et al., 2000), its reduction in the crude synaptosomal fraction allows us to hypothesize a reduction in striatal and hippocampal spine density. Interestingly, a decreased striatal expression of transcripts encoding PSD95 in psychiatric patients has been reported (Kristiansen & Meador-Woodruff, 2005). Taken together, we hypothesize that repeated exposure to JWH-018 caused molecular and structural changes that led to a dynamic impairment of striatal and hippocampal glutamate homeostasis in JWH-018-treated mice, as also previously observed following long-term Δ9–THC treatment (Fan et al., 2010).

4.3 | Effect of repeated exposure to JWH-018 on BDNF-related cognitive deficit

Our next step was to focus our attention on the neurotrophin BDNF, known to play a key role both in recognition (Mottarlini et al., 2020) and spatial memory (Poulia et al., 2021) following exposure to drugs of abuse. Our analyses revealed a significant reduction of the BDNF-mediated intracellular pathway in the hippocampus of JWH-018-withdrawn mice. In fact, mBDNF and the phosphorylation of its high affinity receptor trkB, and Akt, one of the main proteins activated by the neurotrophin in drug-withdrawal state (Giannotti et al., 2014), were reduced. Notably, we found also that the levels of Arc/Arg3.1, a reliable index of brain activity also engaged in structural synaptic plasticity (Bramham et al., 2008), were significantly reduced in the hippocampus of JWH-018-withdrawn mice, pointing to hippocampal structural rearrangements as an additional effect of repeated exposure to JWH18. The role of the BDNF system in modulating cognitive deficit is strengthened by the reduced expression of NMDA receptors, whose contribution to recognition memory has been previously established (Iwamura et al., 2016). Of note, available evidence indicates that BDNF is also a major regulator of hippocampal LTP (Leal et al., 2015). This is very interesting considering that, in the current study, a full blockade of the development of early and late LTP occurs together with impairment in BDNF levels and signalling.

4.4 | Effects of repeated exposure to JWH-018 on the endocannabinoid system and dopamine levels

Withdrawal from repeated exposure to JWH-018 induced significant increases in the levels of the two main endocannabinoid ligands, anandamide (AEA) and 2-AG, paralleled by increased amount of their degradative enzymes, in mouse striatum and a significant CB_1 receptor downregulation in the hippocampus. The evidence of an increased neuronal excitability seen in electrophysiological studies in the hippocampus may be related indirectly to this CB_1 downregulation. Indeed, it has been recently demonstrated that, in neocortical neurons, the activation of CB_1 receptors inhibits voltage gated sodium channels, reducing with high efficacy the neuronal excitability (Steiger et al., 2023).

Prolonged activation of cannabinoid receptors has been shown to lead to decreased endocannabinoid contents in the striatum and decreased receptor binding in most of the CB_1 receptor containing areas (Di Marzo et al., 2000; Rubino et al., 2000). In the 2 weeks after the last JWH-018 injection, we may hypothesize the occurrence of homeostatic changes in the brain that led to the recovery of CB_1 receptor levels in the striatum, but not in the hippocampus, thus suggesting a regional selectivity for the different effects, as already reported in Romero et al. (1998). Moreover, homeostatic changes may also be responsible for the huge increase in striatal AEA levels and the milder elevation in 2-AG, that the brain attempts to deal with by increasing their degradative enzymes. Interestingly, this picture of increased AEA levels in the striatum seems to fit well with the behavioural and neurochemical profile present in JWH-018-treated mice. Indeed, high levels of AEA in the striatum may activate **TRPV1** channels that, in turn, facilitate glutamatergic transmission (Musella et al., 2009). Accordingly, we found a significant increase in K^+-evoked glutamate efflux in JWH-018 mice (see above). Moreover, intracerebroventricular administration of AEA increases locomotor activity (Murillo-Rodríguez et al., 1998) and acute amphetamine administration (a pharmacological manipulation known to increase dopamine in the striatum, see for example Lai et al., 2013), induces hyperlocomotion and elevates AEA in the striatum (Thiemann et al., 2008), features that are also observed in JWH-018-treated mice. Likewise, the increase of the dopamine levels in the striatum could underlie the impairments seen in the tail suspension test, the social dominance test, and the PPI (Bilel et al., 2019). Yet we suggest that these behavioural impairments are triggered by an imbalance of neurotransmitters such as dopamine that is related to an impairment of the endocannabinoid system, and could manifest as psychotic symptoms in human (Shrivastava et al., 2015). In fact, it is generally accepted that excess dopamine transmission, which primary involves the striatum and limbic structures, plays a relevant role in the pathogenesis of psychosis (Dandash et al., 2017; Howes & Shatalina., 2022).

The CB_1 receptor downregulation still present in the hippocampus 15 days after the last JWH-018 injection may play a role in the memory impairment described in the drug-treated mice. Indeed, CB_1 receptor signalling in hippocampal glutamatergic neurons seems to play a fundamental role in the enhancement of learning and memory induced by exercise, through a pathway involving increased BDNF production and dendritic spine density (Wang & Han, 2020). We may hypothesize that the decrease in hippocampal CB_1 receptors may be related to the decreased BDNF production in JWH-treated mice, thus leading to impaired memory in the novel object recognition (NOR) test.

5 | CONCLUSION

The present findings reveal that repeated exposure to JWH-018 followed by long-term drug discontinuation delineates psychotic-like symptoms accompanied by evidence of social and cognitive deficit. These effects may be ascribed, at least partially, to defects in neuroplasticity that appears to be triggered by activation of CB_1 receptors. We are aware that a limitation of our study is that prolonged intraperitoneal administration of an equivalent dose in humans might be associated with severe toxic effects that will limit the translational significance of the results of the present study. However, due to methodological difficulties including the fact that SCBs induced bradypnea, the use of inhalation chambers might not be suitable for repeated administration of high doses of JWH-018. Thus, further studies will be necessary to directly translate the present results to humans. Another limitation is undoubtedly related to the fact that we used male mice only; this is indeed critical because differences in the behavioural and pharmaco-toxicological responses induced by either natural or synthetic cannabinoids in male and female subjects have been proposed (Fattore et al., 2020; Rubino & Parolaro, 2011; Silva et al., 2016). Despite these limitations, the results of the present study may have broad implications that range between drug abuse and schizophrenia and may contribute to explain, at least partially, the comorbidity between these two disorders.

AUTHOR CONTRIBUTIONS

Sabrine Bilel: Data curation (equal); writing—original draft (equal); writing—review and editing (equal). **Erica Zamberletti:** Data curation (equal); writing—original draft (equal); writing—review and editing (equal). **Lucia Caffino:** Data curation (equal); writing—original draft (equal); writing—review and editing (equal). **Micaela Tirri:** Data curation (equal); formal analysis (equal); writing—review and editing (equal). **Francesca Mottarlini:** Data curation (equal); formal analysis (equal); methodology (equal). **Raffaella Arfè:** Data curation (equal); formal analysis (equal); methodology (equal). **Mario Barbieri:** Data curation (equal); formal analysis (equal); methodology (equal). **Sarah Beggiato:** Data curation (equal); methodology (equal); writing—original draft (equal); writing—review and editing (equal). **Federica Boccuto:** Data curation (equal); formal analysis (equal); methodology (equal). **Tatiana Bernardi:** Data curation (equal); formal analysis (equal); methodology (equal). **Sara Casati:** Data curation (equal); formal analysis (equal); methodology (equal). **Anna Teresa Brini:** Data curation (equal); formal analysis (equal); methodology (equal). **Daniela Parolaro:** Conceptualization (equal); investigation (equal); writing—original draft (equal). **Luca Ferraro:** Conceptualization (equal); investigation (equal); supervision (equal); writing—original draft (equal); writing—review and editing (equal). **Fabio Fumagalli:** Conceptualization (equal); supervision (equal); writing—original draft (equal); writing—review and editing (equal). **Matteo Marti:** Conceptualization (equal); supervision (equal); writing—original draft (equal); writing—review and editing (equal).

ACKNOWLEDGEMENTS

This research has been funded by the Department of Anti-Drug Policies, Presidency of the Council of Ministers, Italy (project: 'Effects of NPS: development of a multicentric research for the information enhancement of the Early Warning System' to MM), by local funds from the University of Ferrara (FAR 2020 and FAR 2021 to MM) and by MIUR Progetto Eccellenza.

CONFLICT OF INTEREST STATEMENT

The authors declare no conflict of interest in relation to the work herein described.

DATA AVAILABILITY STATEMENT

The data that support the findings of this study are available from the corresponding author upon reasonable request. Some data may not be made available because of privacy or ethical restrictions.

DECLARATION OF TRANSPARENCY AND SCIENTIFIC RIGOUR

This Declaration acknowledges that this paper adheres to the principles for transparent reporting and scientific rigour of preclinical research as stated in the BJP guidelines for Design and Analysis, Immunoblotting and Immunochemistry, and Animal Experimentation, and as recommended by funding agencies, publishers and other organizations engaged with supporting research.

ORCID

Lucia Caffino https://orcid.org/0000-0001-8045-3146
Francesca Mottarlini https://orcid.org/0000-0001-8172-1384
Sara Casati https://orcid.org/0000-0002-5049-7321
Fabio Fumagalli https://orcid.org/0000-0002-8814-7706
Matteo Marti https://orcid.org/0000-0001-8751-2882

REFERENCES

Alexander, S. P., Christopoulos, A., Davenport, A. P., Kelly, E., Mathie, A., Peters, J. A., Veale, E. L., Armstrong, J. F., Faccenda, E., Harding, S. D., Pawson, A. J., Southan, C., Davies, J. A., Abbracchio, M. P., Alexander, W., al-Hosaini, K., Bäck, M., Barnes, N. M., Bathgate, R., … Ye, R. D. (2021). The concise guide to pharmacology 2021/22: G protein-coupled receptors. *British Journal of Pharmacology*, *178*(Suppl 1), S27–S156. https://doi.org/10.1111/bph.15538

Alexander, S. P., Fabbro, D., Kelly, E., Mathie, A., Peters, J. A., Veale, E. L., Armstrong, J. F., Faccenda, E., Harding, S. D., Pawson, A. J., Southan, C., Davies, J. A., Beuve, A., Brouckaert, P., Bryant, C., Burnett, J. C., Farndale, R. W., Friebe, A., Garthwaite, J., … Waldman, S. A. (2021). THE CONCISE GUIDE TO PHARMACOLOGY 2021/22: Catalytic receptors. *British Journal of Pharmacology*, *178*(S1), S264–S312. https://doi.org/10.1111/bph.15541

Alexander, S. P., Fabbro, D., Kelly, E., Mathie, A., Peters, J. A., Veale, E. L., Armstrong, J. F., Faccenda, E., Harding, S. D., Pawson, A. J., Southan, C., Davies, J. A., Boison, D., Burns, K. E., Dessauer, C., Gertsch, J., Helsby, N. A., Izzo, A. A., Koesling, D., … Wong, S. S. (2021). THE CONCISE GUIDE TO PHARMACOLOGY 2021/22: Enzymes. *British Journal of Pharmacology*, *178*(S1), S313–S411. https://doi.org/10.1111/bph.15542

Alexander, S. P., Mathie, A., Peters, J. A., Veale, E. L., Striessnig, J., Kelly, E., Armstrong, J. F., Faccenda, E., Harding, S. D., Pawson, A. J., Southan, C., Davies, J. A., Aldrich, R. W., Attali, B., Baggetta, A. M., Becirovic, E., Biel, M., Bill, R. M., Catterall, W. A., … Zhu, M. (2021). THE CONCISE GUIDE TO PHARMACOLOGY 2021/22: Ion channels. *British Journal of Pharmacology*, *178*(S1), S157–S245. https://doi.org/10.1111/bph.15539

Alexander, S. P. H., Roberts, R. E., Broughton, B. R. S., Sobey, C. G., George, C. H., Stanford, S. C., … Ahluwalia, A. (2018). Goals and practicalities of immunoblotting and immunohistochemistry: A guide for submission to the British Journal of pharmacology. *British Journal of Pharmacology*, *175*(3), 407–411. https://doi.org/10.1111/bph.14112

Anderson, W. W., & Collingridge, G. L. (2007). Capabilities of the WinLTP data acquisition program extending beyond basic LTP experimental functions. *Journal of Neuroscience Methods*, *162*(1-2), 346–356. https://doi.org/10.1016/j.jneumeth.2006.12.018

Barbieri, M., Ossato, A., Canazza, I., Trapella, C., Borelli, A. C., Beggiato, S., Rimondo, C., Serpelloni, G., Ferraro, L., & Marti, M. (2016). Synthetic cannabinoid JWH-018 and its halogenated derivatives JWH-018-cl and JWH-018-Br impair novel object recognition in mice: Behavioral, electrophysiological and neurochemical evidence. *Neuropharmacology*, *109*, 254–269. https://doi.org/10.1016/j.neuropharm.2016.06.027

Barbieri, M., Tirri, M., Bilel, S., Arfè, R., Corli, G., Marchetti, B., Caruso, L., Soukupova, M., Cristofori, V., Serpelloni, G., & Marti, M. (2022). Synthetic cannabinoid JWH-073 alters both acute behavior and in vivo/vitro electrophysiological responses in mice. *Frontiers in Psychiatry*, *13*, 953909. https://doi.org/10.3389/fpsyt.2022.953909

Barrionuevo, G., & Brown, T. H. (1983). Associative long-term potentiation in hippocampal slices. *Proceedings of the National Academy of Sciences of the United States of America*, *80*(23), 7347–7351. https://doi.org/10.1073/pnas.80.23.7347

Basavarajappa, B. S., & Subbanna, S. (2014). CB1 receptor-mediated signaling underlies the hippocampal synaptic, learning, and memory deficits following treatment with JWH-081, a new component of spice/K2 preparations. *Hippocampus*, *24*(2), 178–188. https://doi.org/10.1002/hipo.22213

Bilel, S., Tirri, M., Arfè, R., Ossato, A., Trapella, C., Serpelloni, G., Neri, M., Fattore, L., & Marti, M. (2020). Novel halogenated synthetic cannabinoids impair sensorimotor functions in mice. *Neurotoxicology*, *76*, 17–32. https://doi.org/10.1016/j.neuro.2019.10.002

Bilel, S., Tirri, M., Arfè, R., Stopponi, S., Soverchia, L., Ciccocioppo, R., Frisoni, P., Strano-Rossi, S., Miliano, C., De-Giorgio, F., Serpelloni, G., Fantinati, A., De Luca, M. A., Neri, M., & Marti, M. (2019). Pharmacological and behavioral effects of the synthetic cannabinoid AKB48 in rats. *Frontiers in Neuroscience*, *13*, 1163. https://doi.org/10.3389/fnins.2019.01163

Borgan, F., Kokkinou, M., & Howes, O. (2021). The cannabinoid CB1 receptor in schizophrenia. *Biological Psychiatry: Cognitive Neuroscience and Neuroimaging*, *6*(6), 646–659. https://doi.org/10.1016/j.bpsc.2020.06.018

Bramham, C. R., Worley, P. F., Moore, M. J., & Guzowski, J. F. (2008). The immediate early gene arc/arg3.1: Regulation, mechanisms, and function. *The Journal of Neuroscience*, *28*(46), 11760–11767. https://doi.org/10.1523/JNEUROSCI.3864-08.2008

Caffino, L., Mottarlini, F., Mingardi, J., Zita, G., Barbon, A., & Fumagalli, F. (2020). Anhedonic-like behavior and BDNF dysregulation following a single injection of cocaine during adolescence. *Neuropharmacology*, *175*, 108161. https://doi.org/10.1016/j.neuropharm.2020.108161

Caffino, L., Piva, A., Giannotti, G., Di Chio, M., Mottarlini, F., Venniro, M., Yew, D. T., Chiamulera, C., & Fumagalli, F. (2017). Ketamine self-administration reduces the homeostasis of the glutamate synapse in the rat brain. *Molecular Neurobiology*, *54*(9), 7186–7193. https://doi.org/10.1007/s12035-016-0231-6

Canazza, I., Ossato, A., Trapella, C., Fantinati, A., De Luca, M. A., Margiani, G., Vincenzi, F., Rimondo, C., Di Rosa, F., Gregori, A., Varani, K., Borea, P. A., Serpelloni, G., & Marti, M. (2016). Effect of the novel synthetic cannabinoids AKB48 and 5F-AKB48 on 'tetrad', sensorimotor, neurological and neurochemical responses in mice. In vitro and in vivo pharmacological studies. *Psychopharmacology*, *233*(21–22), 3685–3709. https://doi.org/10.1007/s00213-016-4402-y

Celofiga, A., Koprivsek, J., & Klavz, J. (2014). Use of synthetic cannabinoids in patients with psychotic disorders: Case series. *Journal of Dual Diagnosis*, *10*, 168–173. https://doi.org/10.1080/15504263.2014.929364

Chung, E. Y., Cha, H. J., Min, H. K., & Yun, J. (2021). Pharmacology and adverse effects of new psychoactive substances: Synthetic cannabinoid receptor agonists. *Archives of Pharmacal Research*, *44*(4), 402–413. https://doi.org/10.1007/s12272-021-01326-6

Cooper, Z. D. (2016). Adverse effects of synthetic cannabinoids: Management of Acute Toxicity and Withdrawal. *Current Psychiatry Reports*, *18*(5), 52. https://doi.org/10.1007/s11920-016-0694-1

Corli, G., Tirri, M., Arfè, R., Bilel, S., Marchetti, B., Gregori, A., Di Rosa, F., Vincenzi, F., de-Giorgio, F., Borea, P. A., Varani, K., & Marti, M. (2022). Behavioral and binding studies on the quinolinyl ester indoles 5F-PB22 (5F-QUPIC) and BB-22 (QUCHIC) in the mouse model. *Emerging Trends in Drugs, Addictions, and Health*, *2*, 100039. https://doi.org/10.1016/j.etdah.2022.100039

Curtis, M. J., Alexander, S. P. H., Cirino, G., George, C. H., Kendall, D. A., Insel, P. A., Izzo, A. A., Ji, Y., Panettieri, R. A., Patel, H. H., Sobey, C. G., Stanford, S. C., Stanley, P., Stefanska, B., Stephens, G. J., Teixeira, M. M., Vergnolle, N., & Ahluwalia, A. (2022). Planning experiments: Updated guidance on experimental design and analysis and their reporting III. *British Journal of Pharmacology*, *179*(15), 3907–3913. https://doi.org/10.1111/bph.15868

Dandash, O., Pantelis, C., & Fornito, A. (2017). Dopamine, fronto-striato-thalamic circuits and risk for psychosis. *Schizophrenia Research*, *180*, 48–57. https://doi.org/10.1016/j.schres.2016.08.020

Davidson, C., Opacka-Juffry, J., Arevalo-Martin, A., Garcia-Ovejero, D., Molina-Holgado, E., & Molina-Holgado, F. (2017). Spicing up pharmacology: A review of synthetic cannabinoids from structure to adverse events. *Advances in Pharmacology*, *80*, 135–168. https://doi.org/10.1016/bs.apha.2017.05.001

Delint-Ramirez, I., Segev, A., Pavuluri, A., Self, D. W., & Kourrich, S. (2020). Cocaine-induced synaptic redistribution of NMDARs in striatal neurons alters NMDAR-dependent signal transduction. *Frontiers in Neuroscience*, *14*, 698. https://doi.org/10.3389/fnins.2020.00698

Deng, H., Verrico, C. D., Kosten, T. R., & Nielsen, D. A. (2018). Psychosis and synthetic cannabinoids. *Psychiatry Research*, *268*, 400–412. https://doi.org/10.1016/j.psychres.2018.08.012

Di Carlo, P., Punzi, G., & Ursini, G. (2019). Brain-derived neurotrophic factor and schizophrenia. *Psychiatric Genetics*, *29*(5), 200–210. https://doi.org/10.1097/YPG.0000000000000237

Di Marzo, V., Berrendero, F., Bisogno, T., González, S., Cavaliere, P., Romero, J., Cebeira, M., Ramos, J. A., & Fernández-Ruiz, J. J. (2000). Enhancement of anandamide formation in the limbic forebrain and reduction of endocannabinoid contents in the striatum of delta9-tetrahydrocannabinol-tolerant rats. *Journal of Neurochemistry*, *74*(4), 1627–1635. https://doi.org/10.1046/j.1471-4159.2000.0741627.x

El-Husseini, A. E., Schnell, E., Chetkovich, D. M., Nicoll, R. A., & Bredt, D. S. (2000). PSD-95 involvement in maturation of excitatory synapses. *Science*, *290*(5495), 1364–1368. https://doi.org/10.1126/science.290.5495.1364

Ennaceur, A., Neave, N., & Aggleton, J. P. (1997). Spontaneous object recognition and object location memory in rats: The effects of lesions in the cingulate cortices, the medial prefrontal cortex, the cingulum bundle and the fornix. *Experimental Brain Research*, *113*(3), 509–519. https://doi.org/10.1007/PL00005603

Errico, F., Napolitano, F., Squillace, M., Vitucci, D., Blasi, G., de Bartolomeis, A., Bertolino, A., D'Aniello, A., & Usiello, A. (2013). Decreased levels of D-aspartate and NMDA in the prefrontal cortex and striatum of patients with schizophrenia. *Journal of Psychiatric*

Research, *47*(10), 1432–1437. https://doi.org/10.1016/j.jpsychires.2013.06.013

Everts, H. G. J., & Koolhaas, J. M. (1997). Lateral septal vasopressin in rats: Role in social and object recognition? *Brain Research*, *760*, 1–7. https://doi.org/10.1016/S0006-8993(97)00269-2

Every-Palmer, S. (2010). Warning: Legal synthetic cannabinoid-receptor agonists such as JWH-018 may precipitate psychosis in vulnerable individuals. *Addiction*, *105*, 1859–1860. https://doi.org/10.1111/j.1360-0443.2010.03119.x

Every-Palmer, S. (2011). Synthetic cannabinoid JWH-018 and psychosis: An explorative study. *Drug and Alcohol Dependence*, *117*, 152–157. https://doi.org/10.1016/j.drugalcdep.2011.01.012

Fan, N., Yang, H., Zhang, J., & Chen, C. (2010). Reduced expression of glutamate receptors and phosphorylation of CREB are responsible for in vivo Δ9-THC exposure-impaired hippocampal synaptic plasticity. *Journal of Neurochemistry*, *112*, 691–702. https://doi.org/10.1111/j.1471-4159.2009.06489.x

Fantegrossi, W. E., Moran, J. H., Radominska-Pandya, A., & Prather, P. L. (2014). Distinct pharmacology and metabolism of K2 synthetic cannabinoids compared to Delta(9)-THC: Mechanism underlying greater toxicity? *Life Sciences*, *97*, 45–54. https://doi.org/10.1016/j.lfs.2013.09.017

Fattore, L. (2016). Synthetic cannabinoids-further evidence supporting the relationship between cannabinoids and psychosis. *Biological Psychiatry*, *79*, 539–548. https://doi.org/10.1016/j.biopsych.2016.02.001

Fattore, L., & Fratta, W. (2011). Beyond THC: The new generation of cannabinoid designer drugs. *Frontiers in Behavioral Neuroscience*, *5*, 60. https://doi.org/10.3389/fnbeh.2011.00060

Fattore, L., Marti, M., Mostallino, R., & Castelli, M. P. (2020). Sex and gender differences in the effects of novel psychoactive substances. *Brain Sciences*, *10*(9), 606. https://doi.org/10.3390/brainsci10090606

Franklin, K. B. J., & Paxinos, G. (2008). *The mouse brain in stereotactic coordinates* (3rd ed.). New York.

Gemechu, J. M., Sharma, A., Yu, D., Xie, Y., Merkel, O. M., & Moszczynska, A. (2018). Characterization of dopaminergic system in the striatum of young adult Park2−/− knockout rats. *Scientific Reports*, *8*(1), 1517. https://doi.org/10.1038/s41598-017-18526-0

Geyer, M. A., & Braff, D. L. (1987). Startle habituation and sensorimotor gating in schizophrenia and related animal models. *Schizophrenia Bulletin*, *13*(4), 643–668. https://doi.org/10.1093/schbul/13.4.643

Giannotti, G., Caffino, L., Calabrese, F., Racagni, G., Riva, M. A., & Fumagalli, F. (2014). Prolonged abstinence from developmental cocaine exposure dysregulates BDNF and its signaling network in the medial prefrontal cortex of adult rats. *The International Journal of Neuropsychopharmacology*, *17*, 625–634. https://doi.org/10.1017/S1461145713001454

Hoffman, A. F., Lycas, M. D., Kaczmarzyk, J. R., Spivak, C. E., Baumann, M. H., & Lupica, C. R. (2017). Disruption of hippocampal synaptic transmission and long-term potentiation by psychoactive synthetic cannabinoid 'spice' compounds: Comparison with Delta-tetrahydrocannabinol. *Addiction Biology*, *22*, 390–399. https://doi.org/10.1111/adb.12334

Howes, O. D., & Shatalina, E. (2022). Integrating the neurodevelopmental and dopamine hypotheses of schizophrenia and the role of cortical excitation-inhibition balance. *Biological Psychiatry*, *92*(6), 501–513. https://doi.org/10.1016/j.biopsych.2022.06.017

Huffman, J. W., Dai, D., Martin, B. R., & Compton, D. R. (1994). Design, synthesis and pharmacology of cannabimimetic indoles. *Bioorganic & Medicinal Chemistry Letters*, *4*, 563–566. https://doi.org/10.1016/S0960-894X(01)80155-4

Huffman, J. W., Szklennik, P. V., Almond, A., Bushell, K., Selley, D. E., He, H., Cassidy, M. P., Wiley, J. L., & Martin, B. R. (2005). 1-Pentyl-3-phenylacetylindoles, a new class of cannabimimetic indoles. *Bioorganic & Medicinal Chemistry Letters*, *15*, 4110–4113. https://doi.org/10.1016/j.bmcl.2005.06.008

Iwamura, E., Yamada, K., & Ichitani, Y. (2016). Involvement of hippocampal NMDA receptors in retrieval of spontaneous object recognition memory in rats. *Behavioural Brain Research*, *307*, 92–99. https://doi.org/10.1016/j.bbr.2016.03.048

Javitt, D. C., & Zukin, S. R. (1991). Recent advances in the phencyclidine model of schizophrenia. *The American Journal of Psychiatry*, *148*, 1301–1308. https://doi.org/10.1176/ajp.148.10.1301

Konradi, C., & Heckers, S. (2003). Molecular aspects of glutamate dysregulation: Implications for schizophrenia and its treatment. *Pharmacology & Therapeutics*, *97*(2), 153–179. https://doi.org/10.1016/s0163-7258(02)00328-5

Kristiansen, L. V., & Meador-Woodruff, J. H. (2005). Abnormal striatal expression of transcripts encoding NMDA interacting PSD proteins in schizophrenia, bipolar disorder and major depression. *Schizophrenia Research*, *78*(1), 87–93. https://doi.org/10.1016/j.schres.2005.06.012

Lai, C. C., Lee, L. J., & Yin, H. S. (2013). Combinational effects of ketamine and amphetamine on behaviors and neurotransmitter systems of mice. *Neurotoxicology*, *37*, 136–143. https://doi.org/10.1016/j.neuro.2013.04.014

Larson, J., & Munkácsy, E. (2015). Theta-burst LTP. *Brain Research*, *1621*, 38–50. https://doi.org/10.1016/j.brainres.2014.10.034

Leal, G., Afonso, P. M., Salazar, I. L., & Duarte, C. B. (2015). Regulation of hippocampal synaptic plasticity by BDNF. *Brain Research*, *1621*, 82–101. https://doi.org/10.1016/j.brainres.2014.10.019

Li, R. S., Fukumori, R., Takeda, T., Song, Y., Morimoto, S., Kikura-Hanajiri, R., Yamaguchi, T., Watanabe, K., Aritake, K., Tanaka, Y., Yamada, H., Yamamoto, T., & Ishii, Y. (2019). Elevation of endocannabinoids in the brain by synthetic cannabinoid JWH-018: Mechanism and effect on learning and memory. *Scientific Reports*, *9*(1), 9621. https://doi.org/10.1038/s41598-019-45969-4

Lijam, N., Paylor, R., McDonald, M. P., Crawley, J. N., Deng, C. X., Herrup, K., Stevens, K. E., Maccaferri, G., McBain, C. J., Sussman, D. J., & Wynshaw-Boris, A. (1997). Social interaction and sensorimotor gating abnormalities in mice lacking Dvl1. *Cell*, *90*(5), 895–905. https://doi.org/10.1016/s0092-8674(00)80354-2

Lilley, E., Stanford, S. C., Kendall, D. E., Alexander, S. P., Cirino, G., Docherty, J. R., George, C. H., Insel, P. A., Izzo, A. A., Ji, Y., Panettieri, R. A., Sobey, C. G., Stefanska, B., Stephens, G., Teixeira, M., & Ahluwalia, A. (2020). ARRIVE 2.0 and the British Journal of pharmacology: Updated guidance for 2020. *British Journal of Pharmacology*, *177*(16), 3611–3616. https://doi.org/10.1111/bph.15178

Livny, A., Cohen, K., Tik, N., Tsarfaty, G., Rosca, P., & Weinstein, A. (2018). The effects of synthetic cannabinoids (SCs) on brain structure and function. *European Neuropsychopharmacology*, *28*(9), 1047–1057. https://doi.org/10.1016/j.euroneuro.2018.07.095

Maldonado, R., Cabañero, D., & Martín-García, E. (2020). The endocannabinoid system in modulating fear, anxiety, and stress. *Dialogues in Clinical Neuroscience*, *22*(3), 229–239. https://doi.org/10.31887/DCNS.2020.22.3/rmaldonado

Mason, N. L., Theunissen, E. L., Hutten, N. R. P. W., Tse, D. H. Y., Toennes, S. W., Stiers, P., & Ramaekers, J. G. (2019). Cannabis induced increase in striatal glutamate associated with loss of functional corticostriatal connectivity. *European Neuropsychopharmacology: the Journal of the European College of Neuropsychopharmacology*, *29*(2), 247–256. https://doi.org/10.1016/j.euroneuro.2018.12.003

Morini, R., Mlinar, B., Baccini, G., & Corradetti, R. (2011). Enhanced hippocampal long-term potentiation following repeated MDMA treatment in dark-agouti rats. *European Neuropsychopharmacology*, *21*(1), 80–91. https://doi.org/10.1016/j.euroneuro.2010.07.007

Mottarlini, F., Racagni, G., Brambilla, P., Fumagalli, F., & Caffino, L. (2020). Repeated cocaine exposure during adolescence impairs recognition memory in early adulthood: A role for BDNF signaling in the perirhinal cortex. *Developmental Cognitive Neuroscience*, *43*, 100789. https://doi.org/10.1016/j.dcn.2020.100789

Murillo-Rodríguez, E., Sánchez-Alavez, M., Navarro, L., Martínez-González, D., Drucker-Colín, R., & Prospéro-García, O. (1998). Anandamide modulates sleep and memory in rats. *Brain Research*, *812*(1-2), 270–274. https://doi.org/10.1016/s0006-8993(98)00969-x

Musella, A., De Chiara, V., Rossi, S., Prosperetti, C., Bernardi, G., Maccarrone, M., & Centonze, D. (2009). TRPV1 channels facilitate glutamate transmission in the striatum. *Molecular and Cellular Neurosciences*, *40*(1), 89–97. https://doi.org/10.1016/j.mcn.2008.09.001

Oka, M., Ito, K., Koga, M., & Kusumi, I. (2020). Changes in subunit composition of NMDA receptors in animal models of schizophrenia by repeated administration of methamphetamine. *Progress in Neuro-Psychopharmacology & Biological Psychiatry*, *103*, 109984. https://doi.org/10.1016/j.pnpbp.2020.109984

Orsolini, L., Chiappini, S., Papanti, D., De Berardis, D., Corkery, J. M., & Schifano, F. (2019). 2019 the bridge between classical and 'synthetic'/chemical psychoses: Towards a clinical, psychopathological, and therapeutic perspective. *Frontiers in Psychiatry*, *10*, 851. https://doi.org/10.3389/fpsyt.2019.00851

Ossato, A., Canazza, I., Trapella, C., Vincenzi, F., de Luca, M. A., Rimondo, C., Varani, K., Borea, P. A., Serpelloni, G., & Marti, M. (2016). Effect of JWH-250, JWH-073 and their interaction on 'tetrad', sensorimotor, neurological and neurochemical responses in mice. *Progress in Neuro-Psychopharmacology & Biological Psychiatry*, *67*, 31–50. https://doi.org/10.1016/j.pnpbp.2016.01.007

Ossato, A., Uccelli, L., Bilel, S., Canazza, I., Di Domenico, G., Pasquali, M., Pupillo, G., De Luca, M. A., Boschi, A., Vincenzi, F., Rimondo, C., Beggiato, S., Ferraro, L., Varani, K., Borea, P. A., Serpelloni, G., De-Giorgio, F., & Marti, M. (2017). Psychostimulant effect of the synthetic cannabinoid JWH-018 and AKB48: Behavioral, neurochemical, and dopamine transporter scan imaging studies in mice. *Frontiers in Psychiatry*, *8*, 130. https://doi.org/10.3389/fpsyt.2017.00130

Ossato, A., Vigolo, A., Trapella, C., Seri, C., Rimondo, C., Serpelloni, G., & Marti, M. (2015). JWH-018 impairs sensorimotor functions in mice. *Neuroscience*, *300*, 174–188. https://doi.org/10.1016/j.neuroscience.2015.05.021

Percie du Sert, N., Hurst, V., Ahluwalia, A., Alam, S., Avey, M. T., Baker, M., Browne, W. J., Clark, A., Cuthill, I. C., Dirnagl, U., Emerson, M., Garner, P., Holgate, S. T., Howells, D. W., Karp, N. A., Lazic, S. E., Lidster, K., MacCallum, C. J., Macleod, M., … Würbel, H. (2020). The ARRIVE guidelines 2.0: Updated guidelines for reporting animal research. *PLoS Biology*, *18*(7), e3000410. https://doi.org/10.1371/journal.pbio.3000410

Pérez-Otaño, I., & Ehlers, M. D. (2004). Learning from NMDA receptor trafficking: Clues to the development and maturation of glutamatergic synapses. *Neuro-Signals*, *13*, 175–189. https://doi.org/10.1159/000077524

Pintori, N., Castelli, M. P., Miliano, C., Simola, N., Fadda, P., Fattore, L., Scherma, M., Ennas, M. G., Mostallino, R., Flore, G., De Felice, M., Sagheddu, C., Pistis, M., Di Chiara, G., & De Luca, M. A. (2021). Repeated exposure to jwh-018 induces adaptive changes in the mesolimbic and mesocortical dopamine pathways, glial cells alteration and behavioural correlates. *British Journal of Pharmacology*, *178*, 3476–3497. https://doi.org/10.1111/bph.15494

Poleszak, E., Wośko, S., Sławińska, K., Wyska, E., Szopa, A., Świąder, K., Wróbel, A., Doboszewska, U., Wlaź, P., Wlaź, A., & Serefko, A. (2020). Influence of the CB1 and CB2 cannabinoid receptor ligands on the activity of atypical antidepressant drugs in the behavioural tests in mice. *Pharmacology, Biochemistry, and Behavior*, *188*, 172833. https://doi.org/10.1016/j.pbb.2019.172833

Porsolt, R. D., Bertin, A., & Jalfre, M. (1977). Behavioral despair in mice: A primary screening test for antidepressants. *Archives Internationales de Pharmacodynamie et de Thérapie*, *229*, 327–336.

Poulia, N., Delis, F., Brakatselos, C., Polissidis, A., Koutmani, Y., Kokras, N., Dalla, C., Politis, P. K., & Antoniou, K. (2021). Detrimental effects of adolescent escalating low-dose Δ9 -tetrahydrocannabinol leads to a specific bio-behavioural profile in adult male rats. *British Journal of Pharmacology*, *178*(7), 1722–1736. https://doi.org/10.1111/bph.15394

Powell, C. M., & Miyakawa, T. (2006). Schizophrenia-relevant behavioral testing in rodent models: A uniquely human disorder? *Biological Psychiatry*, *59*(12), 1198–1207. https://doi.org/10.1016/j.biopsych.2006.05.008

Romero, J., Berrendero, F., Manzanares, J., Pérez, A., Corchero, J., Fuentes, J. A., Fernández-Ruiz, J. J., & Ramos, J. A. (1998). Time-course of the cannabinoid receptor down-regulation in the adult rat brain caused by repeated exposure to delta9-tetrahydrocannabinol. *Synapse (New York, N.Y.)*, *30*(3), 298–308. https://doi.org/10.1002/(SICI)1098-2396(199811)30:3<298::AID-SYN7>3.0.CO;2-6

Rubino, T., & Parolaro, D. (2011). Sexually dimorphic effects of cannabinoid compounds on emotion and cognition. *Frontiers in Behavioral Neuroscience*, *5*, 64. https://doi.org/10.3389/fnbeh.2011.00064

Rubino, T., Viganò, D., Massi, P., & Parolaro, D. (2000). Changes in the cannabinoid receptor binding, G protein coupling, and cyclic AMP cascade in the CNS of rats tolerant to and dependent on the synthetic cannabinoid compound CP55,940. *Journal of Neurochemistry*, *75*(5), 2080–2086. https://doi.org/10.1046/j.1471-4159.2000.0752080.x

Seely, K. A., Lapoint, J., Moran, J. H., & Fattore, L. (2012). Spice drugs are more than harmless herbal blends: A review of the pharmacology and toxicology of synthetic cannabinoids. *Progress in Neuro-Psychopharmacology & Biological Psychiatry*, *39*(2), 234–243. https://doi.org/10.1016/j.pnpbp.2012.04.017

Shrivastava, A., Johnston, M., Terpstra, K., & Bureau, Y. (2015). Pathways to psychosis in cannabis abuse. *Clinical Schizophrenia & Related Psychoses*, *9*(1), 30–35. https://doi.org/10.3371/CSRP.SHJO.030813

Silva, L., Black, R., Michaelides, M., Hurd, Y. L., & Dow-Edwards, D. (2016). Sex and age specific effects of delta-9-tetrahydrocannabinol during the periadolescent period in the rat: The unique susceptibility of the prepubescent animal. *Neurotoxicology and Teratology*, *58*, 88–100. https://doi.org/10.1016/j.ntt.2016.02.005

Smaga, I., Wydra, K., Piechota, M., Caffino, L., Fumagalli, F., Sanak, M., & Filip, M. (2021). Cocaine abstinence modulates NMDA receptor subunit expression: An analysis of the GluN2B subunit in cocaine-seeking behavior. *Progress in Neuro-Psychopharmacology & Biological Psychiatry*, *109*, 110248. https://doi.org/10.1016/j.pnpbp.2021.110248

Smaga, I., Zaniewska, M., Gawliński, D., Faron-Górecka, A., Szafrański, P., Cegła, M., & Filip, M. (2017). Changes in the cannabinoids receptors in rats following treatment with antidepressants. *Neurotoxicology*, *63*, 13–20. https://doi.org/10.1016/j.neuro.2017.08.012

Spijker, S. (2011). Dissection of Rodent Brain Regions. In K. Li (Ed.), *Neuroproteomics. Neuromethods* (Vol. 57). Humana Press. https://doi.org/10.1007/978-1-61779-111-6_2

Steiger, L. J., Tsintsadze, T., Mattheisen, G. B., & Smith, S. M. (2023). Somatic and terminal CB1 receptors are differentially coupled to voltage-gated sodium channels in neocortical neurons. *Cell Reports*, *42*(3), 112247. https://doi.org/10.1016/j.celrep.2023.112247

Swerdlow, N. R., Light, G. A., Thomas, M. L., Sprock, J., Calkins, M. E., Green, M. F., Greenwood, T. A., Gur, R. E., Gur, R. C., Lazzeroni, L. C., Nuechterlein, K. H., Radant, A. D., Seidman, L. J., Siever, L. J., Silverman, J. M., Stone, W. S., Sugar, C. A., Tsuang, D. W., Tsuang, M. T., … Braff, D. L. (2018). Deficient prepulse inhibition in schizophrenia in a multi-site cohort: Internal replication and extension. *Schizophrenia Research*, *198*, 6–15. https://doi.org/10.1016/j.schres.2017.05.013

Tai, S., Hyatt, W. S., Gu, C., Franks, L. N., Vasiljevik, T., Brents, L. K., Prather, P. L., & Fantegrossi, W. E. (2015). Repeated administration of phytocannabinoid Δ(9)-THC or synthetic cannabinoids JWH-018 and JWH-073 induces tolerance to hypothermia but not locomotor suppression in mice, and reduces CB1 receptor expression and function in a brain region-specific manner. *Pharmacological Research*, *102*, 22–32. https://doi.org/10.1016/j.phrs.2015.09.006

Theunissen, E. L., Reckweg, J. T., Hutten, N. R. P. W., Kuypers, K. P. C., Toennes, S. W., Neukamm, M. A., Halter, S., & Ramaekers, J. G. (2021). Intoxication by a synthetic cannabinoid (JWH-018) causes cognitive and psychomotor impairment in recreational cannabis users. *Pharmacology, Biochemistry, and Behavior*, *202*, 173118. https://doi.org/10.1016/j.pbb.2021.173118

Theunissen, E. L., Reckweg, J. T., Hutten, N. R. P. W., Kuypers, K. P. C., Toennes, S. W., Neukamm, M. A., Halter, S., & Ramaekers, J. G. (2022). Psychotomimetic symptoms after a moderate dose of a synthetic cannabinoid (JWH-018): Implications for psychosis. *Psychopharmacology*, *239*, 1251–1261. https://doi.org/10.1007/s00213-021-05768-0

Thiemann, G., van der Stelt, M., Petrosino, S., Molleman, A., Di Marzo, V., & Hasenöhrl, R. U. (2008). The role of the CB1 cannabinoid receptor and its endogenous ligands, anandamide and 2-arachidonoylglycerol, in amphetamine-induced behavioural sensitization. *Behavioural Brain Research*, *187*(2), 289–296. https://doi.org/10.1016/j.bbr.2007.09.022

van Amsterdam, J., Brunt, T., & van den Brink, W. (2015). The adverse health effects of synthetic cannabinoids with emphasis on psychosis-like effects. *Journal of Psychopharmacology*, *29*(3), 254–263. https://doi.org/10.1177/0269881114565142

Vigolo, A., Ossato, A., Trapella, C., Vincenzi, F., Rimondo, C., Seri, C., Varani, K., Serpelloni, G., & Marti, M. (2015). Novel halogenated derivates of JWH-018: Behavioral and binding studies in mice. *Neuropharmacology*, *95*, 68–82. https://doi.org/10.1016/j.neuropharm.2015.02.008

Wang, H., & Han, J. (2020). The endocannabinoid system regulates the moderate exercise-induced enhancement of learning and memory in mice. *The Journal of Sports Medicine and Physical Fitness*, *60*(2), 320–328. https://doi.org/10.23736/S0022-4707.19.10235-6

Wu, Q., Huang, J., & Wu, R. (2021). Drugs based on NMDAR hypofunction hypothesis in schizophrenia. *Frontiers in Neuroscience*, *15*, 641047. https://doi.org/10.3389/fnins.2021.641047

Zamberletti, E., Prini, P., Speziali, S., Gabaglio, M., Solinas, M., Parolaro, D., & Rubino, T. (2012). Gender-dependent behavioral and biochemical effects of adolescent delta-9-tetrahydrocannabinol in adult maternally deprived rats. *Neuroscience*, *204*, 245–257. https://doi.org/10.1016/j.neuroscience.2011.11.038

Zawilska, J. B., & Wojcieszak, J. (2014). Spice/K2 drugs-more than innocent substitutes for marijuana. *The International Journal of Neuropsychopharmacology*, *17*, 509–525. https://doi.org/10.1017/S1461145713001247

Zhang, X. Y., Liang, J., Chen, D. C., Xiu, M. H., Yang, F. D., Kosten, T. A., & Kosten, T. R. (2012). Low BDNF is associated with cognitive impairment in chronic patients with schizophrenia. *Psychopharmacology*, *222*(2), 277–284. https://doi.org/10.1007/s00213-012-2643-y

Zimmermann, U. S., Winkelmann, P. R., Pilhatsch, M., Nees, J. A., Spanagel, R., & Schulz, K. (2009). Withdrawal phenomena and dependence syndrome after the consumption of 'spice gold'. *Deutsches Ärzteblatt International*, *106*, 464–467. https://doi.org/10.3238/arztebl.2009.0464

Zucchini, S., Buzzi, A., Barbieri, M., Rodi, D., Paradiso, B., Binaschi, A., Coffin, J. D., Marzola, A., Cifelli, P., Belluzzi, O., & Simonato, M. (2008). Fgf-2 overexpression increases excitability and seizure susceptibility but decreases seizure-induced cell loss. *The Journal of Neuroscience*, *28*(49), 13112–13124. https://doi.org/10.1523/JNEUROSCI.1472-08.2008

SUPPORTING INFORMATION

Additional supporting information can be found online in the Supporting Information section at the end of this article.

How to cite this article: Bilel, S., Zamberletti, E., Caffino, L., Tirri, M., Mottarlini, F., Arfè, R., Barbieri, M., Beggiato, S., Boccuto, F., Bernardi, T., Casati, S., Brini, A. T., Parolaro, D., Rubino, T., Ferraro, L., Fumagalli, F., & Marti, M. (2023). Cognitive dysfunction and impaired neuroplasticity following repeated exposure to the synthetic cannabinoid JWH-018 in male mice. *British Journal of Pharmacology*, *180*(21), 2777–2801. https://doi.org/10.1111/bph.16164